Hindawi
Mathematical Problems in Engineering
Volume 2023, Article ID 7795246, 20 pages
https://doi.org/10.1155/2023/7795246

Research Article

Chaotic Dynamics and Control of a Discrete-Time Chen System

Sarker Md. Sohel Rana,[1] **Md. Jasim Uddin**,[1] **P. K. Santra**,[2] **and G. S. Mahapatra**[3]

[1]*Department of Mathematics, University of Dhaka, Dhaka 1000, Bangladesh*
[2]*Abada Nsup School, Abada 711313, Howrah, India*
[3]*Department of Mathematics, National Institute of Technology Puducherry, Karaikal 609609, India*

Correspondence should be addressed to Md. Jasim Uddin; jasim.uddin@du.ac.bd

Received 26 January 2023; Revised 5 May 2023; Accepted 8 May 2023; Published 22 May 2023

Academic Editor: A. K. Alomari

We investigate a discrete-time Chen system. First, we give the topological classifications of the fixed points of this system. Then, we analytically show that the discrete Chen system underlies a Neimark–Sacker (NS) bifurcation and period doubling (PD) under specific parametric circumstances. We confirm the existence of a PD and NS bifurcation via the explicit PD-NS bifurcation criterion and determine the direction of both bifurcations with the help of center manifold theory. We performed numerical simulations to confirm our analytical results. Furthermore, we use the 0-1 chaos test to quantify whether there is chaos in the system or not. At the end, the hybrid control strategy and the OGY (Ott, Grebogi, and Yorke) method are applied to eliminate chaotic trajectories of the system.

1. Introduction

A dynamical system is referred to as a system that changes over time. Today, a mathematical model linked to dynamical systems is used in fields such as weather prediction, ecosystem regulation, heart rate control, power system collapse prevention, and biological applications to human psychiatry, among others. A dynamical system can be divided into continuous dynamical systems and discrete dynamical systems. While many academics have focused on and conducted in-depth investigations into systems bifurcation in continuous dynamical systems, only a few studies have focused on systems bifurcation in discrete dynamical systems. In the continuous dynamical system, many renowned researchers [1–5] have extensively investigated three or higher dimensional. In 1963, Lorenz [2] made the discovery of a 3-D chaotic system while studying the weather model for atmospheric convection. His classical pioneering work inspired scientists to investigate several 3-D chaotic systems. Lü et al. [3] and Ueta and Chen [5] constructed a new critical chaotic system by anticontrol technique in the Lorenz system [2]. These systems are known as Lü system and Chen's system, respectively. Qualitative analysis of these empirical works found many dynamical properties, including local bifurcations, chaotic, periodic, quasiperiodic orbits, and route to chaos. They also obtained super-critical and subcritical bifurcation conditions around positive equilibriums. A novel 3-D chaotic system [4] is investigated to increase the complexity of the chaotic system and the precision of weak signal detection. A 3-D jerk dynamical system examined in [1], which can be utilized as an analog simulator for experiments made in a lab. This work investigated several dramatic and uncommon bifurcation situations, such as those with multiple attractors, symmetry-recovering crises, and basins of attraction for a variety of coexisting attractors. However, many exploratory works have suggested that discrete-time models are more suitable compared to the differential equation model, since the discrete-time model reveals rich chaotic dynamics and gives effective computational models for numerical simulations [6–23]. These researches explored unpredicted properties, including the emergence of (PD-NS) bifurcations and chaos phenomena either numerically or by the applications of normal form theory. These studies focused solely on three-dimensional discrete systems.

Recently, a very short number of contributions have been dedicated to the study of the dynamics of three-dimensional discrete systems [24–31]. For example, discrete-time epidemic models SIR, SEIR, and hypertensive or diabetic exposed to COVID-19 discussed in [24, 26, 28, 32], respectively. In [30], the authors investigated a discrete financial system. In [29], the authors studied a discrete chaotic system. In these works, the researchers concentrated their effort to determine the direction and stability of the PD and NS bifurcations by using explicit PD-NS bifurcation criterion, center manifold theory, and bifurcation theory. The studies in [27] investigated discrete population models. In [25], dynamics of the discrete three-species food chain model is studied through NS bifurcation. These studies used only explicit PD-NS bifurcations criterion and numerical simulations for the existence of PD and NS bifurcations. In nonlinear field research, chaos theory has recently attracted a lot of attention. Chaos is strongly hooked into the initial conditions for the answer trajectories, or the exponential aberration in solution trajectories for little differences within the initial conditions in a discrete system.

In this paper, we consider the Chen system [5]:

$$\begin{aligned} \dot{x} &= a(y - x), \\ \dot{y} &= (c - a)x - xz + cy, \\ \dot{z} &= xy - bz. \end{aligned} \tag{1}$$

In system (1), $x, y, z \in \mathbb{R}$ are the state variables denoting the rate of convective overtuning, the horizontal temperature difference, and the vertical temperature difference, respectively. The parameters $a, b, c \in \mathbb{R}^+$ in the system represent the Prandtl number, the Rayleigh number, and some physical proportions of the region under study, and for a more detailed description of these parameters, we refer to ref [33].

One potential application of the Chen system is weather prediction. The chaotic behavior of the system can help to model complex atmospheric phenomena, such as the formation and movement of storm systems. By simulating the behavior of the Chen system under various initial conditions, researchers can generate forecasts for weather patterns with greater accuracy than traditional methods. This has the potential to greatly benefit industries such as agriculture, transportation, and emergency response, which rely on accurate weather predictions to make important decisions.

Another example is the application of the Chen system in biological research. The chaotic dynamics of the system can be used to model complex biological systems, such as neural networks in the brain. By simulating the behavior of the Chen system, researchers can gain insights into how these systems operate and potentially develop new treatments for neurological disorders.

Overall, the Chen system's broad application prospects make it an exciting area of research with the potential to revolutionize a variety of fields.

In order to obtain the discrete Chen system with integral step size δ, the forward Euler approach is used as follows:

$$\begin{pmatrix} x \\ y \\ z \end{pmatrix} \longrightarrow \begin{pmatrix} x + \delta(a(y - x)) \\ y + \delta((c - a)x - xz + cy) \\ z + \delta(xy - bz) \end{pmatrix} = \begin{pmatrix} f_1(x, y, z) \\ f_2(x, y, z) \\ f_3(x, y, z) \end{pmatrix}. \tag{2}$$

In a discrete system, both the PD and NS bifurcations play a significant role in the generation of critical chaotic dynamics and trigger a route to chaos. The objective of this work is to analyze systematically the conditions for the occurrence of PD and NS bifurcations using an explicit PD-NS bifurcation criterion and to determine the stability and direction of both bifurcations using applications of bifurcation theory.

The remainder of this paper is structured as follows. Section 2 explores the topological classifications of fixed points. In Section 3, we analytically discuss that under a certain parametric condition, system (2) undergoes PD or NS bifurcations. In Section 4, we present the dynamics of system (2) numerically including diagrams of bifurcations, phase portraits, and maximum Lyapunov exponents (MLEs) to validate our analytical findings. We also use the 0 – 1 chaos test to confirm the existence of chaos in the system. In Section 5, we implement hybrid control strategy and the OGY method to stabilize chaos of the uncontrolled system. In Section 6, we present a short discussion.

2. Existence and Local Stability Analysis of Fixed Points

The following system of equations solutions represents the fixed points of system (2):

$$\begin{aligned} x &= f_1(x, y, z), \\ y &= f_2(x, y, z), \\ z &= f_3(x, y, z). \end{aligned} \tag{3}$$

Lemma 1

(i) There is only one fixed point in the system for any variation of the parameter values $E_0 = (0, 0, 0)$

(ii) If $a - 2c < 0$*, then the system has three fixed points* E_0, $E_\pm = (\pm\sqrt{-b(a - 2c)}, \pm\sqrt{-b(a - 2c)}, -a + 2c)$

The Jacobian matrix of system (2) evaluated at $E(x, y, z)$ is as follows:

$$J(E) = \begin{pmatrix} 1-a\delta & a\delta & 0 \\ -(a-c+z)\delta & 1+c\delta & -x\delta \\ y\delta & x\delta & 1-b\delta \end{pmatrix} = (j_{kl}), \quad k,l = 1,2,3. \tag{4}$$

The eigenvalues of the matrix $J(E)$ are the roots of the following characteristic equation:

$$P(\mu) := \mu^3 + \vartheta_2\mu^2 + \vartheta_1\mu + \vartheta_0 = 0, \tag{5}$$

where

$$\vartheta_2 = -tr(J),$$
$$\vartheta_1 = \begin{vmatrix} j_{11} & j_{12} \\ j_{21} & j_{22} \end{vmatrix} + \begin{vmatrix} j_{22} & j_{23} \\ j_{32} & j_{33} \end{vmatrix} + \begin{vmatrix} j_{11} & j_{13} \\ j_{31} & j_{33} \end{vmatrix} \tag{6}$$
$$\vartheta_0 = -|J|.$$

We begin by outlining the following Lemma regarding the prerequisites that must be met for stability near a fixed point of system (2)

Lemma 2 [34]. *Suppose that $\vartheta_2, \vartheta_1, \vartheta_0 \in \mathbb{R}$. Then, each root μ of the following equation has to follow the necessary and sufficient conditions*

$$\mu^3 + \vartheta_2\mu^2 + \vartheta_1\mu + \vartheta_0 = 0, \tag{7}$$

to satisfy $|\mu| < 1$ are $|\vartheta_2 + \vartheta_0| < 1 + \vartheta_1, |\vartheta_2 - 3\vartheta_0| < 3 - \vartheta_1$, and ${\vartheta_0}^2 + \vartheta_1 - \vartheta_0\vartheta_2 < 1$.

Now, the topological classifications of system (2) around a fixed points E_0 and E_+ are given as follows.

At E_0, the Jacobian matrix $J(E_0)$ has eigenvalues $\mu_{1,2} = 1/2\,(2 - a\delta + c\delta \pm \sqrt{\delta^2(c+a)^2 - 12a^2}), \mu_3 = 1 - b\delta$, and $\mu_{1,2}$ satisfies the following equation:

$$\mu^2 - (2 + \breve{\Upsilon}\delta)\mu + \left(1 + \breve{\Upsilon}\delta + \breve{\Theta}\delta^2\right) = 0, \tag{8}$$

where $\breve{\Upsilon} = c - a$, $\breve{\Theta} = a^2 - 2ac$. We discuss the following Lemma regarding the bifurcation behavior of system (2) around the fixed point E_0.

Lemma 3. *For every parameter value selection, the fixed point E_0 is a*

– sink if $(i)\,\breve{\Upsilon}^2 - 4\breve{\Theta} \geq 0, \delta < \min\left\{2/b, -\breve{\Upsilon} - \sqrt{\breve{\Upsilon}^2 - 4\breve{\Theta}}/\breve{\Theta}\right\}$
$(ii)\,\breve{\Upsilon}^2 - 4\breve{\Theta} < 0, \delta < \min\left\{2/b, -\breve{\Upsilon}/\breve{\Theta}\right\}$
– source if $(i)\,\breve{\Upsilon}^2 - 4\breve{\Theta} \geq 0, \delta < \max\left\{2/b, -\breve{\Upsilon} - \sqrt{\breve{\Upsilon}^2 - 4\breve{\Theta}}/\breve{\Theta}\right\}$
$(ii)\,\breve{\Upsilon}^2 - 4\breve{\Theta} < 0, \delta < \max\left\{2/b, -\breve{\Upsilon}/\breve{\Theta}\right\}$
– nonhyperbolic if $(i)\,\breve{\Upsilon}^2 - 4\breve{\Theta} \geq 0, \delta = 2/b$, or $\delta = -\breve{\Upsilon} - \sqrt{\breve{\Upsilon}^2 - 4\breve{\Theta}}/\breve{\Theta}$
$(ii)\,\breve{\Upsilon}^2 - 4\breve{\Theta} < 0, \delta = -\breve{\Upsilon}/\breve{\Theta}$

Let

$$\mathrm{FB}_{E_0} = \left\{(a,b,c,\delta):\ \delta = \frac{-\breve{\Upsilon} \pm \sqrt{\breve{\Upsilon}^2 - 4\breve{\Theta}}}{\breve{\Theta}}, \delta \neq \frac{2}{b}, \breve{\Upsilon}^2 - 4\breve{\Theta} \geq 0\right\}. \tag{9}$$

Then, system (2) experiences a PD bifurcation at E_0 when the parameters (a,b,c,δ) fluctuate within a narrow region of FB_0. Let

$$\mathrm{NSB}_{E_0} = \left\{(a,b,c,\delta):\ \delta = -\frac{\breve{\Upsilon}}{\breve{\Theta}}, \breve{\Upsilon}^2 - 4\breve{\Theta} < 0\right\}, \tag{10}$$

then system (2) experience a NS bifurcation at E_0 if the parameters (a,b,c,δ) change around the set NSB_{E_0}. Now, the eigenvalues of the matrix $J(E_+)$ satisfy the following equation:

$$P(\mu) := \mu^3 + \kappa_{e2}\mu^2 + \kappa_{e1}\mu + \kappa_{e0} = 0, \tag{11}$$

where

$$\kappa_{e2} = -3 + \delta(a+b-c),$$
$$\kappa_{e1} = 3 - 2\delta(a-c) + b\delta(-2 + c\delta),$$
$$\kappa_{e0} = -1 - c\delta - 2a^2b\delta^3 + b\delta(1 - c\delta) + a\delta\left(1 + 4bc\delta^2\right). \tag{12}$$

The following Lemma is provided for stability condition of the fixed point E_+.

Lemma 4. *The fixed point E_+ of system (2) is locally asymptotically stable if and only if the coefficients $\kappa_{e2}, \kappa_{e1}, \kappa_{e0}$ of E_+ of (6) satisfy $|\kappa_{e2} + \kappa_{e0}| < 1 + \kappa_{e1}, |\kappa_{e2} - 3\kappa_{e0}| < 3 - \kappa_{e1}$ and ${\kappa_{e0}}^2 + \kappa_{e1} - \kappa_{e0}\kappa_{e2} < 1$.*

3. Analysis of Bifurcations

In this section, we will discuss the existence, direction, and stability analysis of PD and NS bifurcations near the fixed point E_0 and E_+ by using an explicit PD-NS bifurcation criterion without computing the eigenvalues of the respective system and bifurcation theory [35–37]. We consider δ as the bifurcation parameter, otherwise stated.

3.1. NS Bifurcation around E_0. When $\breve{\Upsilon}^2 - 4\breve{\Theta} < 0$ and the parameters $(a,b,c,\delta) \in \mathrm{NSB}_{E_0}$, then the eigenvalues of the system (2) are

$$\begin{aligned}\mu_{1,2} &= 1 + \frac{\breve{\Upsilon}\delta}{2} \pm \frac{i\delta}{2}\sqrt{4\breve{\Theta} - \breve{\Upsilon}^2} \\ &= \alpha \pm i\beta, \\ \mu_3 &= 1 - b\delta.\end{aligned} \tag{13}$$

Let $\delta = \delta_{NS} = -\breve{\Upsilon}/\breve{\Theta}$, then we have

$$\begin{aligned}\left|\mu_{1,2}(\delta_{NS})\right| &= \sqrt{1 + \breve{\Upsilon}\delta_{NS} + \breve{\Theta}\delta_{NS}^2} \\ &= 1, \\ \mu_3(\delta_{NS}) &= 1 + \frac{b(-a+c)}{a(a-2c)}.\end{aligned} \tag{14}$$

Moreover, the transversality and nonresonance conditions yield

$$\begin{aligned}\left.\frac{d\left|\mu_i(\delta)\right|}{d\delta}\right|_{\delta=\delta_{NS}} &= -\frac{\breve{\Upsilon}}{2} \neq 0 \\ -(2 + \breve{\Upsilon}\delta)|_{\delta=\delta_{NS}} \neq 2, 3 &\Longrightarrow \mu_{1,2}^k \neq 1, k = 1, 2, 3, 4.\end{aligned} \tag{15}$$

Theorem 5. *Suppose (15) holds and $l_1(\delta_{NS}) \neq 0$, then NS bifurcation at a fixed point $E_0(0,0,0)$ for system (2) if δ changes its value in a small neighborhood of NSB_{E_0}. Moreover, if $l_1(\delta_{NS}) < 0$ (resp.$l_1(\delta_{NS}) > 0$), then there is a smooth closed invariant curve that bifurcates from E_0 and the bifurcation is subcritical, either attracting or repelling (resp. super-critical).*

Proof. System (2) can be written as

$$X = A(\delta)X + F, \tag{16}$$

where $F = \begin{pmatrix} 0 \\ -xz\delta \\ xy\delta \end{pmatrix}$.

Then, by [35], we write system (16) as

$$X_{n+1} = AX_n + \frac{1}{2}B(X_n, X_n) + \frac{1}{6}C(X_n, X_n, X_n) + O\left(X_n^4\right), \tag{17}$$

where

$$\begin{aligned}B(x,y) &= \begin{pmatrix} B_1(x,y) \\ B_2(x,y) \\ B_3(x,y) \end{pmatrix}, \\ C(x,y,u) &= \begin{pmatrix} C_1(x,y,u) \\ C_2(x,y,u) \\ C_3(x,y,u) \end{pmatrix},\end{aligned} \tag{18}$$

are the symmetric multilinear functions of $x, y, z, u \in \mathbb{R}^3$, and these functions can be defined by

$$\begin{aligned}B_i(x,y) &= \sum_{j,k=1}^{3} \left.\frac{\partial^2 F_i(v,\delta)}{\partial v_j \partial v_k}\right|_{v=0} x_j y_k, \\ C_i(x,y,u) &= \sum_{j,k,l=1}^{3} \left.\frac{\partial^3 F_i(v,\delta)}{\partial v_j \partial v_k \partial v_l}\right|_{v=0} x_j y_k u_l.\end{aligned} \tag{19}$$

In particular,

$$\begin{aligned}B(x,y) &= \begin{pmatrix} 0 \\ x_3y_1\delta - x_1y_3\delta \\ x_2y_1\delta + x_1y_2\delta \end{pmatrix}, \\ C(x,y,u) &= \begin{pmatrix} 0 \\ 0 \\ 0 \end{pmatrix}.\end{aligned} \tag{20}$$

Let $m_1, m_2 \in \mathbb{C}^3$ be two eigenvectors of $A(\delta_{NS})$ and $A^T(\delta_{NS})$, respectively, such that

$$\begin{aligned}A(\delta_{\mathrm{NS}})m_1 &= \mu(\delta_{\mathrm{NS}})m_1, \\ A(\delta_{\mathrm{NS}})\overline{m_1} &= \overline{\mu}(\delta_{\mathrm{NS}})\overline{m_1}, \\ A^T(\delta_{\mathrm{NS}})m_2 &= \overline{\mu}(\delta_{\mathrm{NS}})m_2, \\ A^T(\delta_{\mathrm{NS}})\overline{m_2} &= \mu(\delta_{\mathrm{NS}})\overline{m_2},\end{aligned} \tag{21}$$

then, we obtain

$$\begin{aligned}m_1 &= \begin{pmatrix} a_1 + ib_1 \\ 1 \\ 0 \end{pmatrix}, \\ m_2 &= \begin{pmatrix} a_2 + ib_2 \\ 1 \\ 0 \end{pmatrix},\end{aligned} \tag{22}$$

where $a_1 = (a+c)/(-2\breve{\Upsilon}), b_1 = \sqrt{\breve{\Upsilon}^2 - \breve{\Theta}}/2\breve{\Upsilon}, a_2 = (a+c)/(-2\breve{\Upsilon}), b_1 = (\sqrt{-\breve{\Upsilon}^2 - \breve{\Theta}})/(2\breve{\Upsilon})$, with $\delta = \delta_{NS}$.

In order to obtain $\langle m_1, m_2\rangle = \sum_{i=1}^{3} m_{1i}\overline{m_{2i}} = 1$, we set the normalized vector $m_2 = \gamma m_2$, where $\gamma = c_1 + id_1, c_1 = ((a_1a_2 + b_1b_2 + 1)/(a_1a_2 + b_1b_2 + 1)^2 + (a_2b_1 - a_1b_2)^2), d_1 = ((a_2b_1 - a_1\ b_2)/(a_1a_2 + b_1b_2 + 1)^2 + (a_2b_1 - a_1b_2)^2)$.

We decompose $X \in \mathbb{R}^3$ as $X = zm_1 + \overline{z}\overline{m_1}$ by considering δ vary near δ_{NS} and for $z \in \mathbb{C}$. The precise formulation of z is $z = \langle m_2, X\rangle$. So, system (16) changed to the following system as a result for the system for $|\delta|$ close to δ_{NS}:

$$z \longmapsto \mu(\delta)z + \widehat{g}(z, \overline{z}, \delta), \tag{23}$$

where $\mu(\delta) = (1 + \widehat{\phi}(\delta))e^{i\theta(\delta)}$ with $\widehat{\phi}(\delta_{\mathrm{NS}}) = 0$ and $\widehat{g}(z, \overline{z}, \delta)$ is a smooth complex-valued function. Applying the Taylor expansion to the function $\widehat{g}$, we obtain

$$\widehat{g}(z, \overline{z}, \delta) = \sum_{k+l\geq 2} \frac{1}{k!l!}\widehat{g}_{kl}(\delta)z^{k-l} \text{ with } \widehat{g}_{kl} \in \mathbb{C}, k, l = 0, 1, \ldots. \tag{24}$$

By using symmetric multilinear vector functions, the Taylor coefficients can be defined as

$$\begin{aligned}
\widehat{g}_{20}(\delta_{\mathrm{NS}}) &= \langle m_2, B(m_1, m_1)\rangle,\\
\widehat{g}_{11}(\delta_{\mathrm{NS}}) &= \langle m_2, B(m_1, \overline{m_1})\rangle,\\
\widehat{g}_{02}(\delta_{\mathrm{NS}}) &= \langle m_2, B(\overline{m_1}, \overline{m_1})\rangle,\\
\widehat{g}_{21}(\delta_{\mathrm{NS}}) &= \langle m_2, C(m_1, m_1, \overline{m_1})\rangle + 2\langle m_2, B\left(m_1, (I_n - A)^{-1}B(m_1, \overline{m_1})\right)\rangle\\
&\quad + \langle m_2, B\left(\overline{m_1}, \left(\mu_1^2 I_n - A\right)^{-1}B(m_1, m_1)\right)\rangle + \frac{\mu_2(1-2\mu_1)}{1-\mu_1}g_{20}g_{11}\\
&\quad + \frac{2}{1-\mu_1}|g_{11}|^2 + \frac{\mu_1}{\mu_1^3 - 1}|g_{02}|^2.
\end{aligned} \tag{25}$$

Then, we obtain $\widehat{g}_{20}(\delta_{\mathrm{NS}}) = 0, \widehat{g}_{11}(\delta_{\mathrm{NS}}) = 0, \widehat{g}_{02}(\delta_{\mathrm{NS}}) = 0, \widehat{g}_{21}(\delta_{\mathrm{NS}}) = -(2\delta)/(b(A_5^2 + B_5^2))\ [(A_4A_5 + B_4B_5) + i(A_5B_4 - A_4B_5)]$, where

$$\begin{aligned}
A_5 &= -1 + \alpha^2 - \beta^2 + b\delta,\\
B_5 &= 2\alpha\beta,\\
A_4 &= A_2A_3 - B_2B_3,\\
B_4 &= A_3B_2 + A_2B_3,\\
A_3 &= a_1\left(-2 + 2\alpha^2 - 2\beta^2 + 3b\delta\right),\\
B_3 &= 4a_1\alpha\beta - bb_1\delta,\\
A_2 &= A_1\alpha + B_1\beta,\\
B_2 &= B_1\alpha - A_1\beta,\\
A_1 &= a_1c_1 + b_1d_1,\\
B_1 &= b_1c_1 - a_1d_1.
\end{aligned} \tag{26}$$

To ensure the direction of NS bifurcation, we require that the coefficient, $l_1(\delta_{\mathrm{NS}})$, does not equal to zero. Hence,

$$\begin{aligned}
l_1(\delta_{\mathrm{NS}}) &= \mathrm{Re}\left(\frac{\mu_2\widehat{g}_{21}}{2}\right) - \mathrm{Re}\left(\frac{(1-2\mu_1)\mu_2{}^2}{2(1-\mu_1)}\widehat{g}_{20}\widehat{g}_{11}\right)\\
&\quad - \frac{1}{2}|\widehat{g}_{11}|^2 - \frac{1}{4}|\widehat{g}_{02}|^2\\
&= -\frac{\delta(A_6A_5 + B_6B_5)}{b\left(A_5^2 + b_5^2\right)}.
\end{aligned} \tag{27}$$

Therefore, $l_1(\delta_{\mathrm{NS}}) = -(\delta(A_6A_5 + B_6B_5))/(b(A_5^2 + b_5^2))$, where

$$\begin{aligned}
A_6 &= A_1A_3 - B_1B_3,\\
B_6 &= A_3B_1 + A_1B_3.
\end{aligned} \tag{28}$$

Hence, the theorem is proved. □

3.2. Bifurcation Analysis around E_+

3.2.1. PD Bifurcation at E_+: Existence. To investigate the existence of PD bifurcation, we will use the following lemma discussed in [37].

Lemma 6. *The PD bifurcation of system (2) takes place around the fixed point E_+ at $\delta = \delta_F$ if and only if*

$$\begin{aligned}
&1 - \kappa_{e1} + \kappa_{e0}(\kappa_{e2} - \kappa_{e0}) > 0,\\
&1 + \kappa_{e1} - \kappa_{e0}(\kappa_{e2} + \kappa_{e0}) > 0,\\
&1 + \kappa_{e2} + \kappa_{e1} + \kappa_{e0} > 0,\\
&1 - \kappa_{e2} + \kappa_{e1} - \kappa_{e0} = 0,\\
&1 + \kappa_{e0} > 0, 1 - \kappa_{e0} > 0,
\end{aligned} \tag{29}$$

and $(\sum_{i=1}^{n}(-1)^{n-i}\iota_i')/(\sum_{i=1}^{n}(-1)^{n-i}(n-i+1)\iota_{i-1}) = (\kappa_{e2}{}' - \kappa_{e1}{}' + \kappa_{e0}{}')/(3 - 2\kappa_{e2} + \kappa_{e1}) \neq 0$, *where $\kappa_{e2}, \kappa_{e1}, \kappa_{e0}$ are given as in (12) and $\kappa_i' = d\kappa_i/d\delta|_{\delta=\delta_F}$ with*

$$\begin{aligned}
\delta_F &= \frac{1}{3}\left[-\frac{c}{a^2 - 2ac} - \frac{\left(-6a(a-2c)(a+b-c) - bc^2\right)}{\left(a(a-2c)\left(H_1 + \sqrt{H_2}\right)^{1/3}\right)} + \frac{1}{ab(a-2c)}\left(H_1 + \sqrt{H_2}\right)^{1/3}\right],\\
H_1 &= -54a^4b^2 + 207a^3b^2c - 9a^2b^3c - 189a^2b^2c^2 + 18ab^3c^2 - 18ab^2c^3 - b^3c^3,\\
H_2 &= b^3\left(-\left(6a(a-2c)(a+b-c) + bc^2\right)^3 + bH_3\right),\\
H_3 &= \left(54a^4 - 207a^3c - 18a(b-c)c^2 + bc^3 + 9a^2c(b+21c)\right)^2.
\end{aligned} \tag{30}$$

If the values of the system parameters vary in a small neighborhood of the set

$$FB_{E_+} = \{(a,b,c,\delta)\colon \delta = \delta_F, a,b,c>0\}, \tag{31}$$

then one of the eigenvalues of the characteristic (11) is $\mu_3(\delta_F) = -1$, and the other two are $|\mu_{1,2}(\delta_F)| \neq \pm 1$, and therefore, system (2) underlies a PD bifurcation around the fixed point E_+.

3.2.2. PD Bifurcation around E_+: Direction and Stability. Here, the direction of PD bifurcation will be determined by the applications of center manifold theory [35]. We consider the fixed point $E_+(\sqrt{-b(a-2c)}, \sqrt{-b(a-2c)}, -a+2c)$ of system (2) with arbitrary parameters $(a,b,c,\delta) \in FB_{E_+}$.

Theorem 7. *Suppose equation (32) holds well and $l_2(\delta_F) \neq 0$. If δ changes its value around the bifurcation point, then a PD bifurcation will occur for system (2) at the fixed point $E_+(x^+, y^+, z^+)$. Furthermore, if $l_2(\delta_F) < 0$ (resp. $l_2(\delta_F) > 0$), then there exists unstable (resp. stable) period-2 points that bifurcate from $E_+(x^+, y^+, z^+)$.*

Proof. Let $\delta = \delta_F$, then the eigenvalues of $J(E_+)$ are

$$|\mu_i(\delta_F)| \neq \pm 1, \mu_3(\delta_F) = -1, i = 1, 2. \tag{32}$$

Next, we use the transformation $\hat{x} = x - x^+, \hat{y} = y - y^+, \hat{z} = z - z^+$, where $x^+ = y^+ = \sqrt{-b(a-2c)}, z^+ = -a + 2c$ and set $A(\delta_F) = J(E_+)$. Next, we transfer the fixed point E_+ of system (2) to the origin since the symmetric multilinear functions are not associated with a fixed point. Therefore, these bilinear and trilinear functions for flip bifurcation will remain unchanged as defined in (18).

Consider two eigenvectors $n_1, n_2 \in \mathbb{R}^3$ of A for eigenvalue $\mu_3(\delta_F) = -1$ such that

$$\begin{aligned} A(\delta_F)n_1 &= -n_1, \\ A^T(\delta_F)n_2 &= -n_2, \end{aligned} \tag{33}$$

where n_1 and n_2 must satisfy the inner product property $\langle n_1, n_2\rangle = 1$. Therefore, the sign of $l_2(\delta_F)$ can be used to determine the direction of PD bifurcation, which is calculated by

$$\begin{aligned} l_2(\delta_F) = {} & \frac{1}{6}\langle n_2, C(n_1,n_1,n_1)\rangle \\ & - \frac{1}{2}\langle n_2, B\big(n_1, (A-I)^{-1}B(n_1,n_1)\big)\rangle. \end{aligned} \tag{34}$$

Hence, the theorem is proved. □

3.2.3. NS Bifurcation around E_+: Existence. We will introduce the following Lemma in [36, 37] for the existence of NS bifurcation with the help of explicit Flip-NS bifurcation criterion.

Lemma 8. *The NS bifurcation of system (2) occurs around the fixed point E_+ at $\delta = \delta_{NS}$ if and only if*

$$\begin{aligned} 1 - \kappa_{e1} + \kappa_{e0}(\kappa_{e2} - \kappa_{e0}) &= 0, \\ 1 + \kappa_{e1} - \kappa_{e0}(\kappa_{e2} + \kappa_{e0}) &> 0, \\ 1 + \kappa_{e2} + \kappa_{e1} + \kappa_{e0} &> 0, \\ 1 - \kappa_{e2} + \kappa_{e1} - \kappa_{e0} &> 0, \\ \frac{d}{d\delta}(1 - \kappa_{e1} + \kappa_{e0}(\kappa_{e2} - \kappa_{e0}))_{\delta=\delta_{NS}} &\neq 0, \\ \cos(2\pi/l) \neq 1 - \frac{(1 + \kappa_{e2} + \kappa_{e1} + \kappa_{e0})}{(2(1+\kappa_{e0}))}, & l = 3, 4, 5, \ldots, \end{aligned} \tag{35}$$

where $\kappa_{e2}, \kappa_{e1}, \kappa_{e0}$ are given as in (12) with

$$\begin{aligned} \delta_{\mathrm{NS}} &= -\frac{1}{48a^2b(a-2c)^2}\left[16ab(a-2c)c + \frac{K_1}{(K_2 + 3\sqrt{3}\sqrt{K_3})^{1/3}} + 8(K_2 + 3\sqrt{3}\sqrt{K_3})^{1/3}\right], \\ K_1 &= \left(8a^2b(a-2c)^2\left(6a^3 + 6a^2(b-3c) - 12a(b-c)c + bc^2\right)\right), \\ K_2 &= -54a^{10}b^2 + 531a^9b^2c + 8a^3b^3c^6 + 12a^4b^2c^5(-13b + 12c) + 72a^7b^2c^2(b + 56c) \\ &\quad + 6a^5b^2c^4(49b + 216c) - 9a^8b^2c(b + 231c) - a^6b^2c^3(217b + 3816c), \\ K_3 &= \left(-a^8b^3(a-2c)^8\left(\begin{array}{c} 8a^5 - 4a^4(21b + 10c) + bc^2\left(b^2 - 6bc + c^2\right) + 12a^3\left(2b^2 + 25bc + 6c^2\right) \\ + a^2\left(8b^3 - 108b^2c - 203bc^2 - 56c^3\right) + 2ac\left(-8b^3 + 61b^2c - 61bc^2 + 8c^3\right) \end{array}\right)\right). \end{aligned} \tag{36}$$

For parameter perturbation in a small neighborhood of

$$NSB_{E_+} = \{(a, b, c, \delta):\ \delta = \delta_{\mathrm{NS}}, a, b, c > 0\}, \tag{37}$$

two roots (eigenvalues) of the characteristic (11) are complex conjugates that have modulus one and the magnitude of the other root is not equal to one, then system (2) experiences NS bifurcation around E_+.

3.2.4. NS Bifurcation around E_+: Direction and Stability. This section will present the direction of the NS bifurcation with the help of the center manifold theory.

Next, we choose the fixed point $E_+(x^+, y^+, z^+)$ of system (2) with arbitrary parameters $(a, b, c, \delta) \in NSB_{E_+}$.

Theorem 9. *Suppose (38) holds and $l_3(\delta_{\mathrm{NS}}) \neq 0$, then NS bifurcation at a fixed point $E_+(x^+, y^+, z^+)$ for system (2) if δ changes its value in a small neighborhood of NSB_{E_+}. Moreover, if $l_3(\delta_{\mathrm{NS}}) < 0$ (resp.$l_3(\delta_{\mathrm{NS}}) > 0$), then there is a smooth closed invariant curve that bifurcates from E_+ and the bifurcation is subcritical, either attracting or repelling (resp. super-critical).*

Proof. Let $\delta = \delta_{\mathrm{NS}}$, then the matrix $J(E_+)$ has the eigenvalues satisfying

$$\left|\mu_i(\delta_{\mathrm{NS}})\right| = 1, \mu_3(\delta_{\mathrm{NS}}) \neq 1, i = 1, 2. \tag{38}$$

For eigenvalues $\mu(\delta_{\mathrm{NS}})$ and $\overline{\mu}(\delta_{\mathrm{NS}})$, let $q_1, q_2 \in \mathbb{C}^3$ be two eigenvectors of $A(\delta_{\mathrm{NS}})$ and $A^T(\delta_{\mathrm{NS}})$, respectively, such that the following conditions hold:

$$\begin{aligned} A(\delta_{\mathrm{NS}})q_1 &= \mu(\delta_{\mathrm{NS}})q_1, \\ A(\delta_{\mathrm{NS}})\overline{q_1} &= \overline{\mu}(\delta_{\mathrm{NS}})\overline{q_1}, \\ A^T(\delta_{\mathrm{NS}})q_2 &= \overline{\mu}(\delta_{\mathrm{NS}})q_2, \\ A^T(\delta_{\mathrm{NS}})\overline{q_2} &= \mu(\delta_{\mathrm{NS}})\overline{q_2}, \end{aligned} \tag{39}$$

and the eigenvector q_1, q_2 must satisfy $\langle q_1, q_2\rangle = \sum_{i=1}^{3} q_{1i}\overline{q_{2i}} = 1$.

The sign of the first Lyapunov coefficient $l_3(\delta_{NS})$ determines the direction of NS bifurcation and is defined in statement (27).

Hence, the theorem is proved. □

4. Numerical Simulations

In this section, we will perform numerical simulations to support our theoretical results for system (2) which includes diagrams of bifurcation, phase portraits, and MLEs. We take parameter values given in Table 1 to investigate bifurcation analysis.

Example 10. We take the values of the parameters as in case (i). We find a fixed point $E_+ = (0, 0, 0)$ and bifurcation point for system (2) is evaluated at $\delta_{NS} = 0.145833$.

Now, at $\delta = \delta_{NS}$, the Jacobian matrix of the system (2) takes the form of

$$A(\delta_F) = \begin{pmatrix} -2.5 & 3.5 & 0 \\ -2.04167 & 2.45833 & 0 \\ 0 & 0 & -0.75 \end{pmatrix}, \tag{40}$$

and the eigenvalues of $A(\delta_F)$ are $\mu_{1,2} = 0.0208333 \pm 0.999783i$ and $\mu_3 = -0.75$ with $|\mu_{1,2}| = 1$.

Also,

$$\begin{aligned} \left.\frac{d|\mu_i(\delta)|}{d\delta}\right|_{\delta=\delta_{\mathrm{NS}}} &= -\frac{\breve{\Upsilon}}{2} \\ &= \frac{a-c}{2} \\ &= 7 \neq 0, \end{aligned} \tag{41}$$

$$-(2 + \breve{\Upsilon}\delta)|_{\delta=\delta_{\mathrm{NS}}} = \frac{1}{24} \neq 2, 3.$$

Let $m_1, m_2 \in \mathbb{C}^3$ be two complex eigenvectors of $A(\delta_{\mathrm{NS}})$ and $A^T(\delta_{\mathrm{NS}})$ corresponding to $\mu_{1,2}$, respectively. Therefore,

$$\begin{aligned} m_1 &\sim (1.21429 - 0.48969i, 1, 0)^T, \\ m_2 &\sim (-.708333 - 0.285652i, 1, 0)^T. \end{aligned} \tag{42}$$

For $\langle m_1, m_2\rangle = 1$, then we can take normalized vector as $m_2 = \gamma m_2$ where $\gamma = 0.5 + 1.2985i$. Then, we get

$$\begin{aligned} m_1 &\sim (1.21429 - 0.48969i, 1, 0)^T, \\ m_2 &\sim (-1.02105i, 0.5 + 1.23985i, 0)^T. \end{aligned} \tag{43}$$

Also, by (25), the Taylor coefficients are $\widehat{g}_{20} = 0, \widehat{g}_{11} = 0, \widehat{g}_{02} = 0, \widehat{g}_{21} = 0.0833333 - 0.273497i$.

From (39), we obtain the Lyapunov coefficient $l_1(\delta_{\mathrm{NS}}) = -0.137587 < 0$. Therefore, the NS bifurcation is supercritical, and the requirements of Theorem 5 are established.

The NS bifurcation diagrams are displayed in Figures 1(a)–1(c) which reveal that the condition of stability for the fixed point E_0 occurs when $\delta < \delta_{\mathrm{NS}}$ and loses its stability at $\delta = \delta_{\mathrm{NS}}$, and there appears an attracting closed invariant curve when $\delta > \delta_{\mathrm{NS}}$. The nonstability of dynamical system is justified with the sign of MLEs (1 (d)).

The phase portraits of system (2) corresponding to the bifurcation diagram shown in Figure 1 are plotted in Figure 2. This figure explicitly illustrates the mechanism of how an invariant smooth closed curve bifurcates from a stable fixed point E_0 when δ changes near its critical value. We noticed that NS bifurcations occur at $\delta = \delta_{\mathrm{NS}}$. When $\delta > \delta_{\mathrm{NS}}$, there appears an invariant closed curve, and further increasing of δ, the NS bifurcation instigates a route to chaos.

Example 11. We take the values of the parameters as in case (ii). We find a fixed point $E_+ = (2.48495, 2.48495, 0.65)$ and bifurcation point for the system (2) is evaluated at $\delta_F = 0.2150920185$.

Now, at $\delta = \delta_F$, the Jacobian matrix of system (2) takes the form

Table 1: Parameter values.

Cases	Parameter range with variation	Fixed parameters	Dynamics of system
(i)	$0.14 \le \delta \le 0.1495$	$a = 24, b = 12, c = 10$	NS bifurcation
(ii)	$0.2 \le \delta \le 0.2302$	$a = 3.45, b = 9.5, c = 2.05$	PD bifurcation
(iii)	$0.01 \le \delta \le 0.037$	$a = 28, b = 55, c = 18$	PD and NS bifurcation
(iv)	$25.5 \le a \le 34$	$b = 78, c = 18, \delta = 0.0264$	NS bifurcation
(v)	$25.5 \le a \le 34, 72 \le b \le 80$	$c = 18, \delta = 0.0264$	NS bifurcation

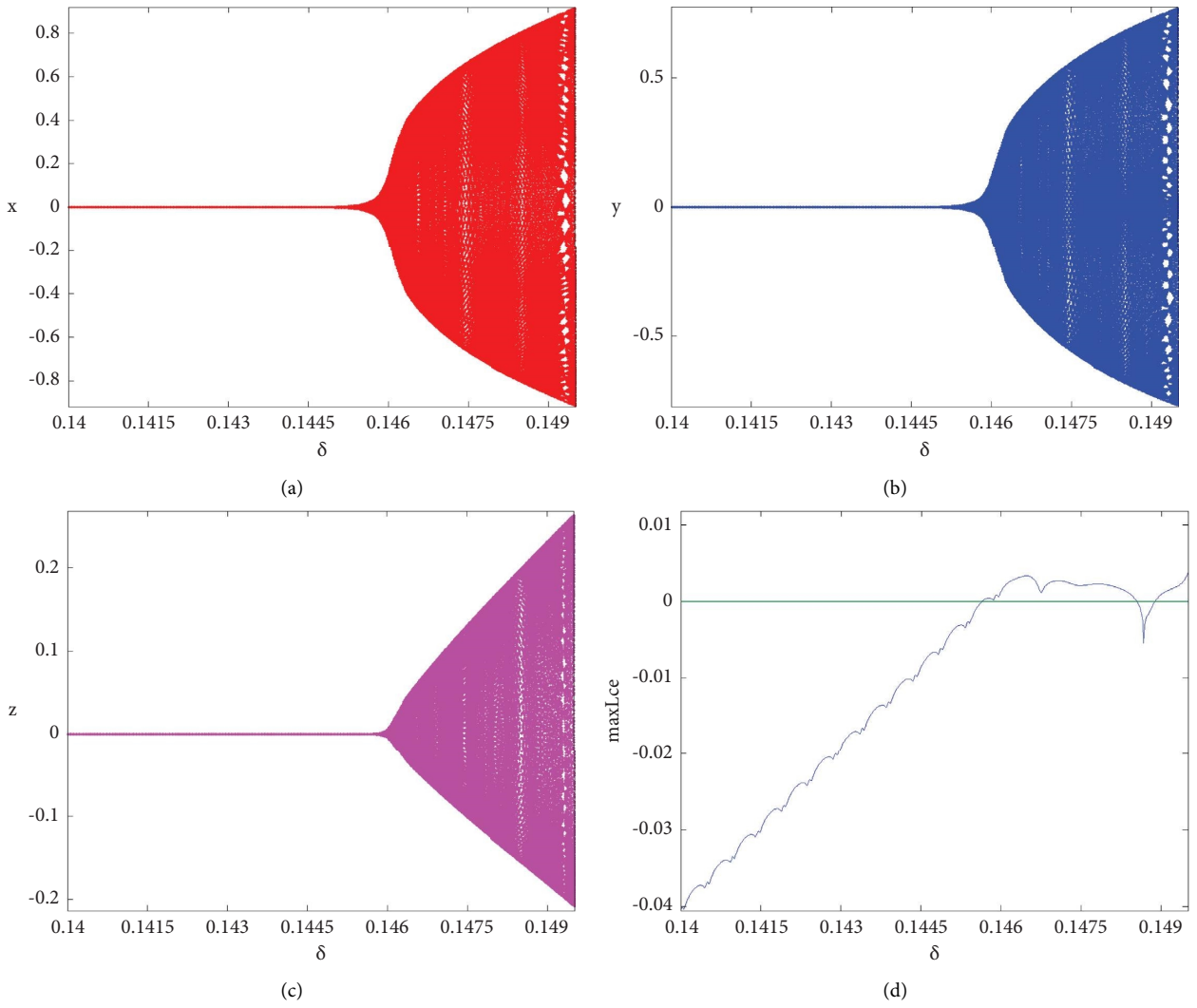

Figure 1: NS bifurcation diagram in (a) (δ, x) plane, (b) (δ, y) plane, (c) (δ, z) plane, (d) MLEs, $(x_0, y_0, z_0) = (0.04, 0.04, 0.04)$.

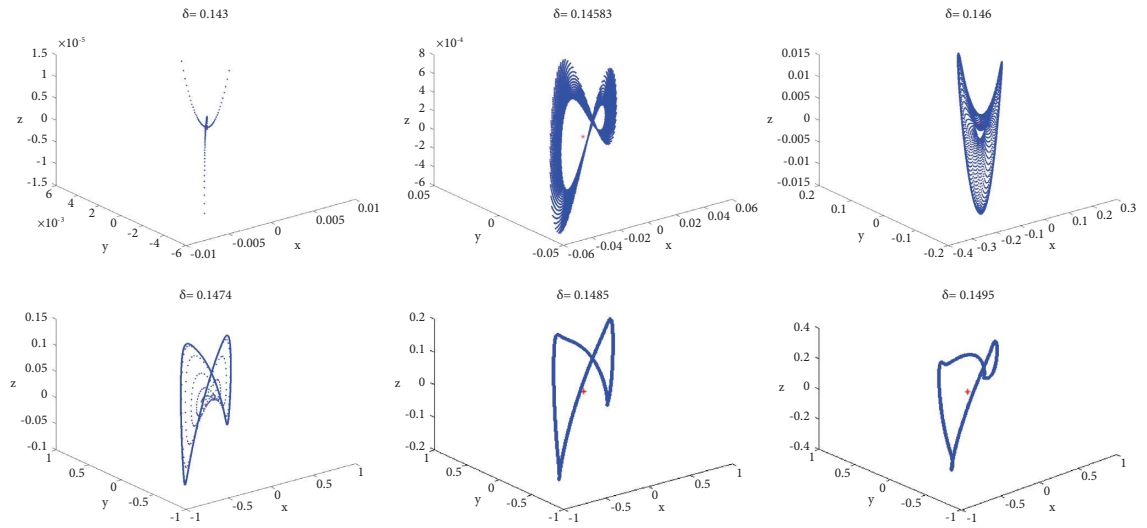

Figure 2: Phase portrait for different values of δ corresponding to Figures 1(a)–1(c). Red $*$ is the fixed point E_0.

$$A(\delta_F) = \begin{pmatrix} 0.257933 & 0.742067 & 0 \\ -0.440939 & 1.44094 & -0.534494 \\ 0.534494 & 0.534494 & -1.04337 \end{pmatrix}, \quad (44)$$

and the eigenvalues of $A(\delta_F)$ are $\mu_{1,2} = 0.827748 \pm 0.426997i$ and $\mu_3 = -1$ with $|\mu_{1,2}| \neq 1$. Moreover,

$$\begin{aligned} 1 - \kappa_{e1} + \kappa_{e0}(\kappa_{e2} - \kappa_{e0}) &= 0.466819 > 0, \\ 1 + \kappa_{e1} - \kappa_{e0}(\kappa_{e2} + \kappa_{e0}) &= 0.0280909 > 0, \\ 1 + \kappa_{e2} + \kappa_{e1} + \kappa_{e0} &= 0.423993 > 0, \\ 1 - \kappa_{e2} + \kappa_{e1} - \kappa_{e0} &= 0, \\ 1 + \kappa_{e0} &= 1.86749 > 0, \\ 1 - \kappa_{e0} &= 0.132506 > 0, \\ \frac{\kappa_{e2}' - \kappa_{e1}' + \kappa_{e0}'}{3 - 2\kappa_{e2} + \kappa_{e1}} &= 9.29835 \neq 0. \end{aligned} \quad (45)$$

This shows that all requirements of Lemma 6 are validated with $(a, b, c, \delta) \in \mathrm{FB}_{E_+}$, and so, PD bifurcation of system (2) exists around E_+ at $\delta = \delta_F$. Next, let the two eigenvectors of $A(\delta_F)$ corresponding to $\mu_3(\delta_F) = -1$, be $m_1, m_2 \in \mathbb{R}^3$, respectively. Then, we obtain

$$\begin{aligned} n_1 &\sim (-0.11377, 0.192859, 0.974609)^T, \\ n_2 &\sim (-0.411773, -0.0737086, 0.908301)^T. \end{aligned} \quad (46)$$

To set $\langle n_1, n_2 \rangle = 1$, we can choose normalized vector as $n_2 = \gamma n_2$ where $\gamma = 1.08948$. Therefore,

$$\begin{aligned} n_1 &\sim (-0.11377, 0.192859, 0.974609)^T, \\ n_2 &\sim (-0.448618, -0.080304, 0.989575)^T. \end{aligned} \quad (47)$$

Then, from statement (34), the Lyapunov coefficient $l_2(\delta_F) = 0.00293263$ is obtained. This guarantees the appropriateness of Theorem 7.

The bifurcation diagrams shown in Figures 3(a)–3(c) express the stability of the fixed point E_+ when $\delta < \delta_F$, lose its stability at $\delta = \delta_F$, and when $\delta > \delta_F$, a period-doubling phenomena trigger chaotic dynamics. The sign of MLEs illustrates instability of system (2) (see Figure 3(d)). The phase portrait in Figure 4 shows the existence of period $-2, -8$ orbits and chaos in system (2)

Example 12. We select the parameters as in case (iii). By calculation, we find a fixed point $E_+ = (20.9762, 20.9762, 8)$ of system (2), and the bifurcation point is obtained as $\delta_{NS} = 0.0220463$.

The Jacobian matrix is evaluated at E_+ is

$$A(\delta_{NS}) = \begin{pmatrix} 0.382705 & 0.617295 & 0 \\ -0.396833 & 1.39683 & -0.462446 \\ 0.462446 & 0.462446 & -0.212544 \end{pmatrix}, \quad (48)$$

and the eigenvalues of $A(\delta_{NS})$ are $\mu_{1,2} = 0.891424 \pm 0.45317i$ and $\mu_3 = -0.215855$ with $|\mu_{1,2}| = 1$.

Furthermore,

$$\begin{aligned} 1 - \kappa_{e1} + \kappa_{e0}(\kappa_{e2} - \kappa_{e0}) &= 0, \\ 1 + \kappa_{e1} - \kappa_{e0}(\kappa_{e2} + \kappa_{e0}) &= 1.90681 > 0, \\ 1 + \kappa_{e2} + \kappa_{e1} + \kappa_{e0} &= 0.264025 > 0, \\ 1 - \kappa_{e2} + \kappa_{e1} - \kappa_{e0} &= 2.9663 > 0, \\ \frac{d}{d\delta}(1 - \kappa_{e1} + \kappa_{e0}(\kappa_{e2} - \kappa_{e0})) &= -14.0993 \neq 0, \\ 1 - \frac{1 + \kappa_{e2} + \kappa_{e1} + \kappa_{e0}}{2(1 + \kappa_{e0})} &= 0.891424. \end{aligned} \quad (49)$$

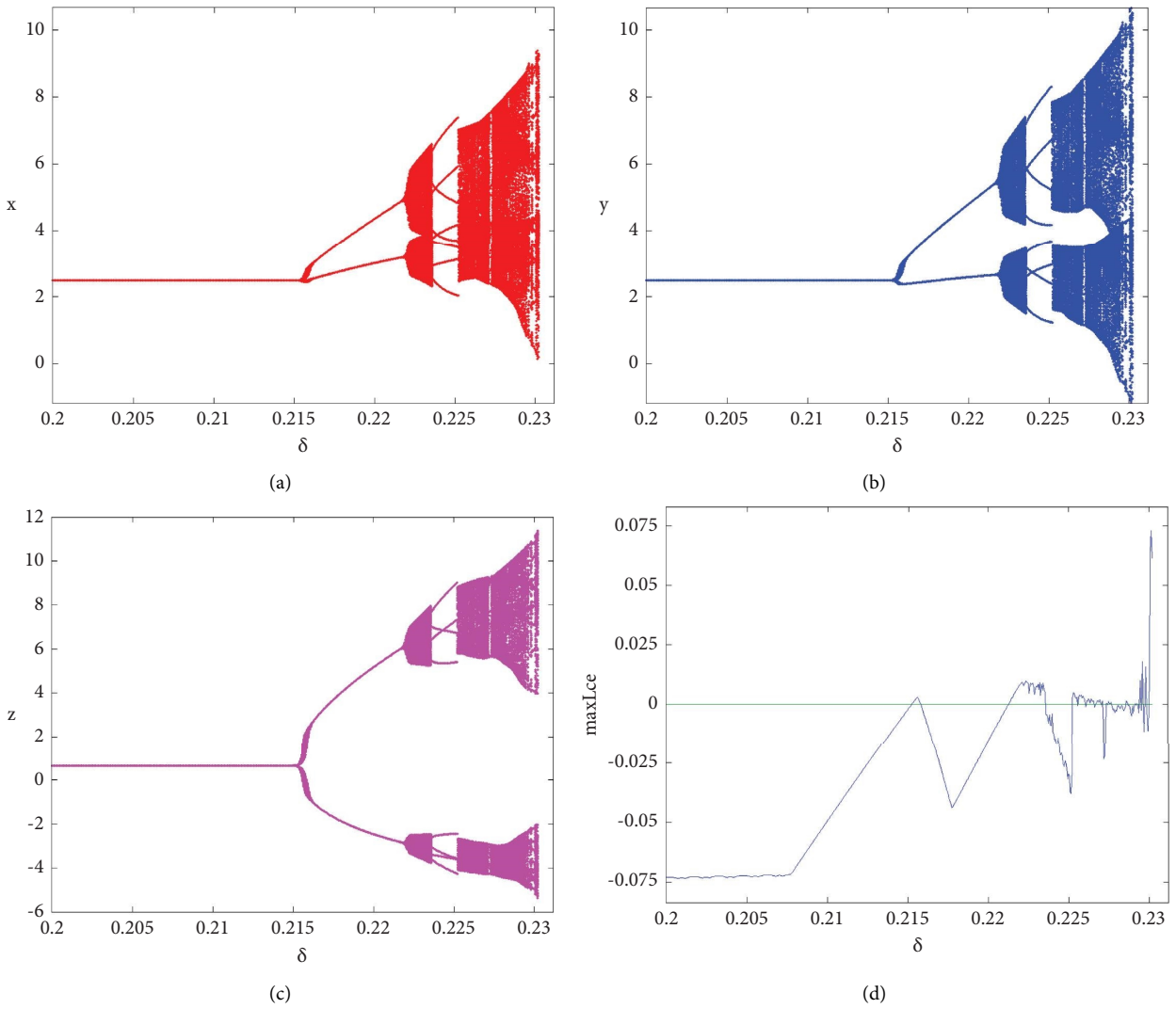

Figure 3: PD bifurcation Diagram in (a) (δ, x) plane, (b) (δ, y) plane, (c) (δ, z) plane, and (d) MLEs related to (a), $(x_0, y_0, z_0) = (2.46495, 2.46495, 0.63)$.

From the resonance condition $\cos(2\pi/l) = 0.891424$, we get $l = \pm 13.3594$.

So, the criterion for the existence of NS bifurcation is fulfilled with $(a, b, c, \delta) \in \mathrm{NSB}_{E_+}$. This confirms the correctness of Lemma 8. Therefore, a NS bifurcation occurs around fixed point E_+ if δ crosses its critical value δ_{NS}.

Let $q_1, q_2 \in \mathbb{C}^3$ be two complex eigenvectors of $A(\delta_{\mathrm{NS}})$ and $A^T(\delta_{\mathrm{NS}})$ corresponding to $\mu_{1,2}$, respectively. Therefore,

$$\begin{aligned} q_1 &\sim (-0.446342 + 0.397604i, -0.659725, -0.338001 + 0.305301i)^T, \\ q_2 &\sim (-0.405371 - 0.45966i, 0.73679, -0.26413 - 0.18423i)^T. \end{aligned} \tag{50}$$

For $\langle q_1, q_2 \rangle = 1$, we can take normalized vector as $q_2 = \gamma q_2$ where $\gamma = -1.02722 - 1.1507i$. Then,

$$\begin{aligned} q_1 &\sim (-0.446342 + 0.397604i, -0.659725, -0.338001 + 0.305301i)^T, \\ q_2 &\sim (-0.112534 + 0.938638i, -0.756843 - 0.84782i, 0.146557 + 0.415308i)^T. \end{aligned} \tag{51}$$

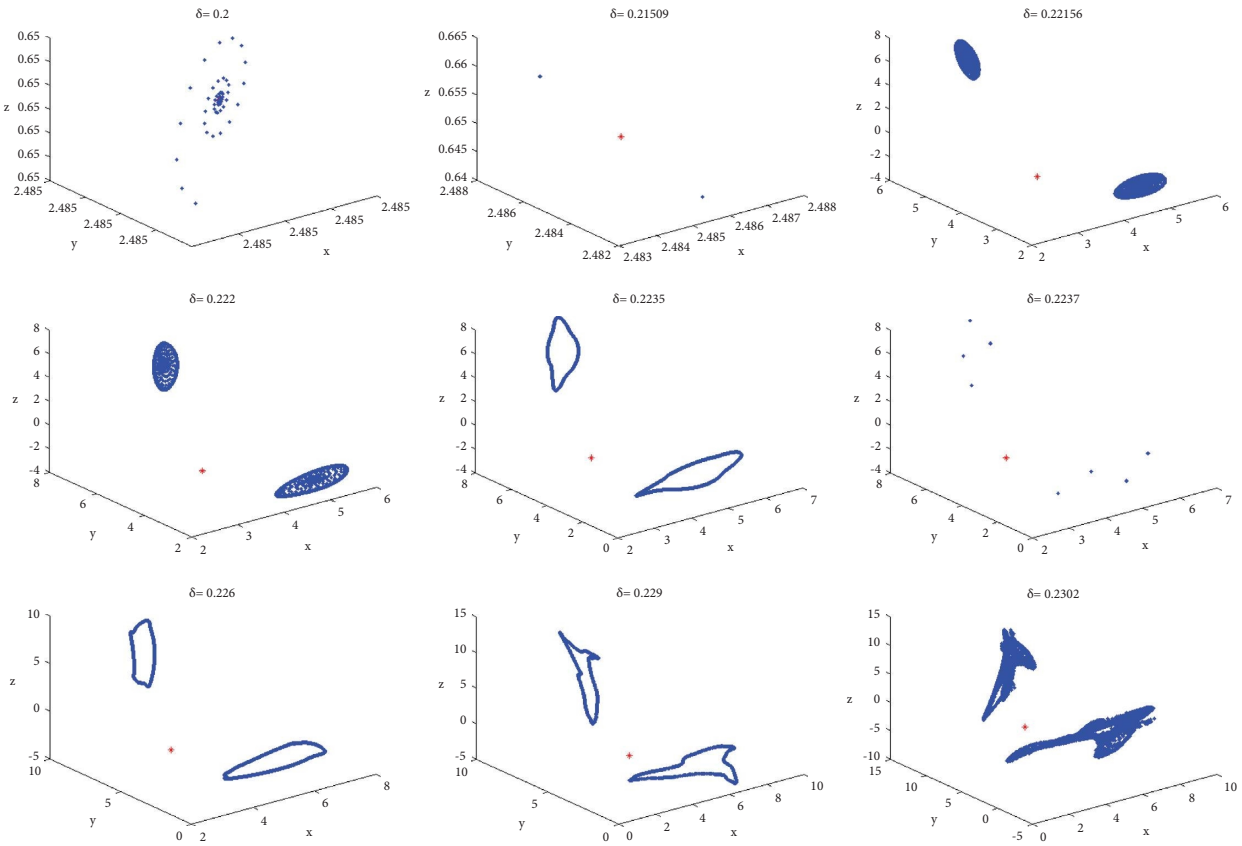

Figure 4: Phase portrait for different values of δ corresponding to Figures 3(a)–3(c). Red $*$ is the fixed point E_+.

Also by statement (25), the Taylor coefficients are $\widehat{g}_{20} = -0.120349 - 0.0172213i$, $\widehat{g}_{11} = 0.0109882 - 0.0155697i$, $\widehat{g}_{02} = 0.0178078 + 0.0042332i$, $\widehat{g}_{21} = 0.000520892 - 0.00138626i$.

From statement (27), we obtain the Lyapunov coefficient $l_3(\delta_{NS}) = -0.000505594 < 0$. As a result, it is established that the NS bifurcation is super-critical, and the conditions of Theorem 9 are met.

The NS bifurcation diagrams are displayed in Figures 5(a)–5(c) which reveal that the stability condition for the positive fixed point E_+ occurs when $\delta < \delta_{\mathrm{NS}}$, loses its stability at $\delta = \delta_{NS}$, and there appears an attracting closed invariant curve when $\delta > \delta_{\mathrm{NS}}$. The MLEs related to Figure 5(a) are shown in Figure 5(d). The nonstability of system dynamics is justified with the sign of MLEs.

The phase portraits of system (2) corresponding to the bifurcation diagram shown in Figure 5 are plotted in Figure 6. We noticed that the appearance of invariant closed curve occurs when $\delta > \delta_{\mathrm{NS}}$ and further changes of δ, and NS bifurcation triggers a route to chaos.

Example 13. For the selection of parameter values in the case (iv) and considering a as bifurcation parameter, we find a fixed point $E_+ = (25.2131, 25.2131, 8.14998)$ of system (2), and bifurcation parameter is calculated at $a_{NS} = 27.85$. Moreover,

$$\begin{aligned} 1 - \kappa_{e1} + \kappa_{e0}(\kappa_{e2} - \kappa_{e0}) &= 0, \\ 1 + \kappa_{e1} - \kappa_{e0}(\kappa_{e2} + \kappa_{e0}) &= 0.0310202 > 0, \\ 1 + \kappa_{e2} + \kappa_{e1} + \kappa_{e0} &= 0.651506 > 0, \\ 1 - \kappa_{e2} + \kappa_{e1} - \kappa_{e0} &= 0.0285954 > 0, \\ \frac{d}{da}(1 - \kappa_{e1} + \kappa_{e0}(\kappa_{e2} - \kappa_{e0})) &= 0.15934 \neq 0, \\ 1 - \frac{1 + \kappa_{e2} + \kappa_{e1} + \kappa_{e0}}{2(1 + \kappa_{e0})} &= 0.836487. \end{aligned} \tag{52}$$

From the resonance condition $\cos(2\pi/l) = 0.836487$, we get $l = \pm 10.8339$.

The correctness of Lemma 8 shows the existence of NS bifurcation at $a = a_{\mathrm{NS}}$. We find the eigenvalue values $\mu_{1,2} = 0.836487 \pm 0.547987i$ and $\mu_3 = -0.99214$ with $|\mu_{1,2}| = 1$ and the Lyapunov coefficient $l_3(a_{NS}) = -0.000554151 < 0$. This makes the NS bifurcation super-critical and supports the validity of Theorem 9.

From the bifurcation diagram Figures 7(a)–7(c) and the phase portrait Figure 8, we noticed that for a small value of a, the system first enters into a chaotic dynamics, and with an increase in a, the chaotic state certainly disappears through an NS bifurcation occurring at $a \sim a_{\mathrm{NS}} = 27.85$. The dynamics of

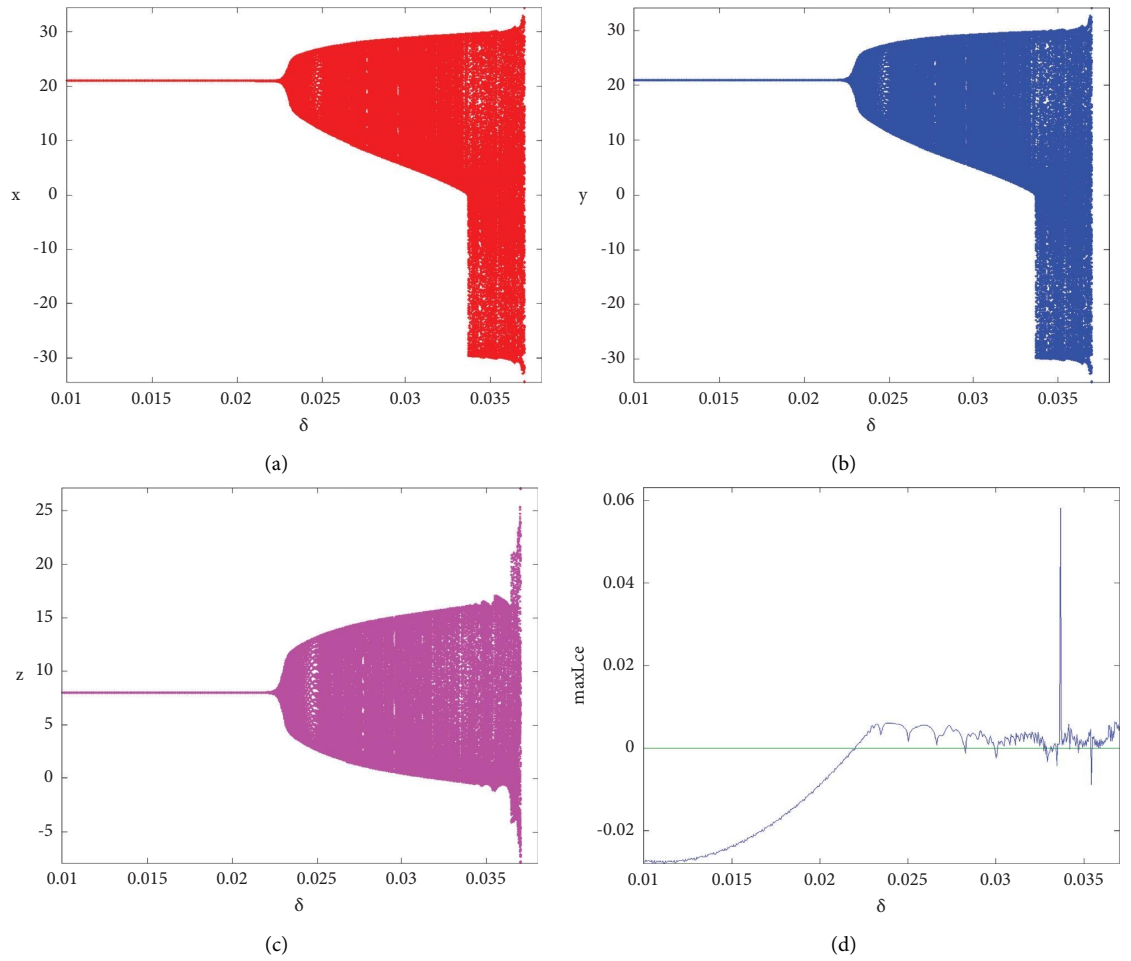

Figure 5: NS bifurcation diagram in (a) (δ, x) plane, (b) (δ, y) plane, (c) (δ, z) plane, (d) MLEs $(x_0, y_0, z_0) = (20.95, 20.95, 7.98)$.

the system then abruptly transitions to a stable state, after which the system experiences a flip bifurcation occurring at $a \sim a_F = 28.4543$, and the period-doubling phenomenon leads to chaos. The sign of MLEs (Figure 7(d)) guarantees that both bifurcations take place in system (2).

Example 14. Two-dimensional parametric space is plotted in Figure 9(a) by taking parameter values as in case (v). The critical values curves of NS and PD bifurcations are shown in that Figure. We observe that for the parameter values of $b < 76$ (approximately), only NS bifurcations occur. Further increase value of b, the system (2) experiences two bifurcations, firstly NS bifurcation and later flip bifurcation. Thereafter, we notice that both bifurcations take place simultaneously at the same point $(a_{\mathrm{NS}-F}, b_{\mathrm{NS}-F}) = (27.8350024, 78.3301)$. In two-dimensional parameter space, the diagrams of bifurcation are presented in Figure 9(b). The instability conditions of system (2) are conformable from the sign of MLEs presented in Figure 9(c).

4.1. 0-1 Chaos Test Algorithm. For $0-1$ chaos test algorithm [38–40], suppose $\theta(n)$ is a measured discrete set of data where $n = 1, 2, 3, \ldots, N$, and the entire amount of the data is N. We pick a number at random $d \in (\pi/5, 4\pi/5)$ and form new coordinates $(q_d(n), r_d(n))$ as follows:

$$q_d(n) = \sum_{j=1}^{n} \theta(j) \cos(\phi(j)),$$
$$r_d(n) = \sum_{j=1}^{n} \theta(j) \sin(\phi(j)), \tag{53}$$

where $\phi(j) = jc + \sum_{i=1}^{j} \theta(j)$, $j = 1, 2, 3, \ldots, n$.

Now, the mean square displacement $C_d(n)$ is now defined as follows:

$$C_d(n) = \lim_{N \longrightarrow \infty} \frac{1}{N} \sum_{j=1}^{N} \left(q_d(j+n) - q_d(j)\right)^2 + \left(r_d(j+n) - r_d(j)\right)^2, \quad n \in \left[1, \frac{N}{10}\right]. \tag{54}$$

The modified mean square displacement is something else we define $C_d(n)$ as follows:

$$C_d(n) = C_d(n) - \left(\lim_{N \longrightarrow \infty} \frac{1}{N} \sum_{j=1}^{N} \theta(j)\right)^2 \frac{1 - \cos nd}{1 - \cos d}. \tag{55}$$

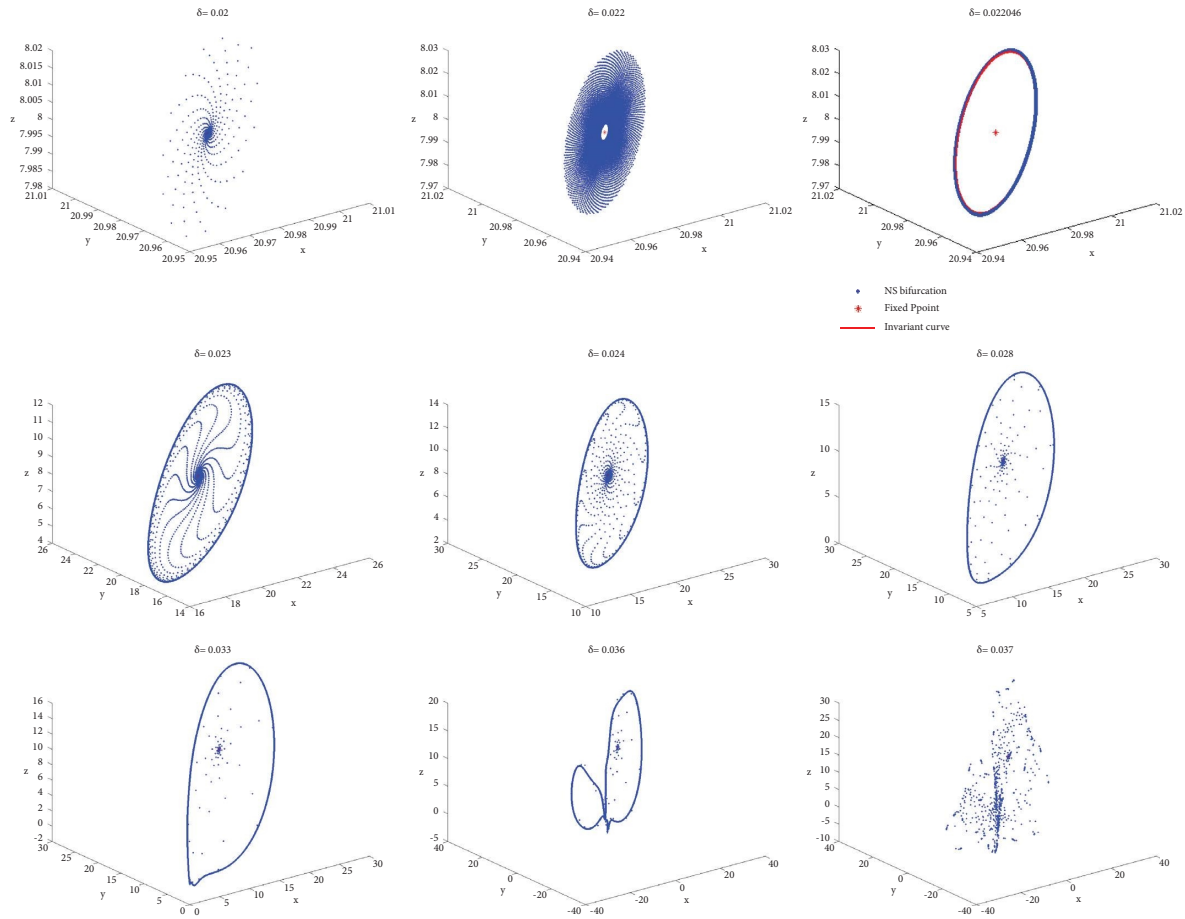

FIGURE 6: Phase portrait for different values of δ corresponding to Figures 5(a)–5(c). Red $*$ is the fixed point E_+.

The median correlation coefficient K value is then described as follows:

$$K = \text{median}(K_d), \tag{56}$$

where

$$K_d = \frac{\text{cov}(\xi_1, \xi_2)}{\sqrt{\text{var}(\xi)\text{var}(\Delta)}} \in [-1, 1], \tag{57}$$

in which $\xi_1 = (1, 2, 3, \ldots, n_{\text{cut}}), \xi_2 = (C_d(1), C_d(2), \ldots, C_d(n_{\text{cut}})), n_{\text{cut}} = \text{round}(N/10)$, and covariance and variance of vectors of length $\overline{n}$ are defined as follows:

$$\begin{aligned} \text{cov}(x, y) &= \frac{1}{\overline{n}} \sum_{j=1}^{\overline{n}} (x(j) - \overline{x})(y(j) - \overline{y}), \\ \overline{x} &= \frac{1}{\overline{n}} \sum_{j=1}^{\overline{n}} x(j), \\ \text{var}(x) &= \text{cov}(x, x). \end{aligned} \tag{58}$$

Now, we can illustrate the output as follows:

(i) The dynamics are consistent (i.e., periodic or quasiperiodic) when $K \approx 0$, whereas $K \approx 1$ suggests that the dynamics are chaotic.

(ii) As opposed to Brownian-like (unbounded) trajectories, which show chaotic dynamics, bounded trajectories on the (q, r) plane show regular dynamics (i.e., periodic or quasiperiodic dynamics).

Example 15. Taking parameters as in case (iii) with $\delta = 0.037$, the system dynamics is chaotic (see in Figure 6), which is consistent with Brownian-like (unbounded) trajectories in new coordinates (q, r)–plane displaying in Figure 10(a) with the value of $K = 0.9774$. The correlation coefficient value curve K versus δ is plotted in Figure 10(b). We find a very nice coincidence between the bifurcation diagram (see in Figure 5) and K diagram showing that with the increase value of δ, the topological properties of system (2) from nonchaotic to chaotic.

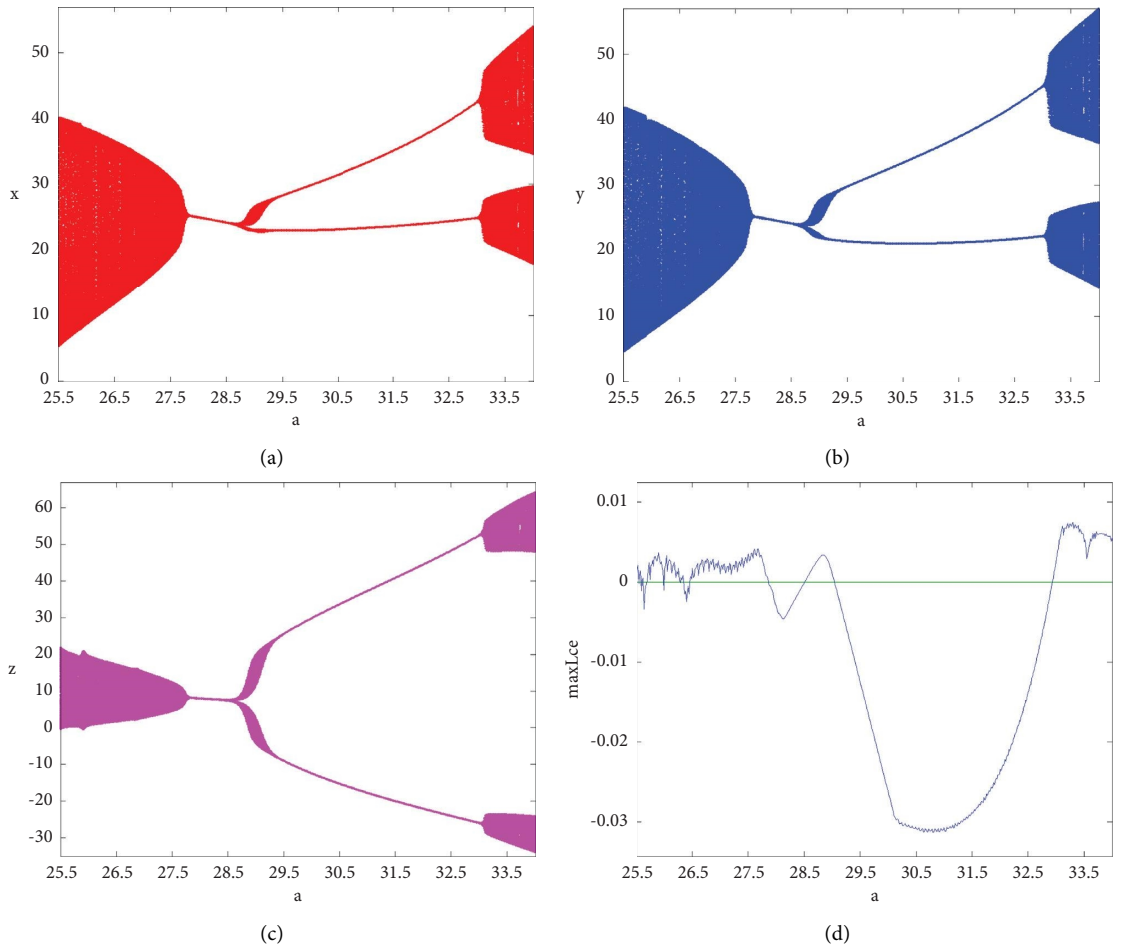

Figure 7: NS bifurcation diagram in (a) (a, x) plane, (b) (a, y) plane, (c) (a, z) plane, and (d) MLEs $(x_0, y_0, z_0) = (25.19, 25.19, 8.10)$.

5. Chaos Control

It can be difficult to keep chaos under control. We introduce a hybrid control [41] and OGY [42] approach to control chaos in the Chen system.The effectiveness, cost, and difficulty of implementing a hybrid control strategy and OGY method to eliminate the chaotic behavior of the Chen system will depend on various factors such as the specific control algorithm used, the complexity of the system, and the hardware and software required for implementation.

However, in general, both the hybrid control strategy and OGY method have been shown to be effective in stabilizing the chaotic behavior of the Chen system in simulation studies and experimental validations. These methods are based on the idea of applying a feedback control signal to the system that counteracts the chaotic behavior and stabilizes the system.

For the cost of implementing these control strategies, it depends on the specific hardware and software requirements, as well as the complexity of the control algorithm used. However, in general, the cost of implementing these methods is not prohibitive, and it is usually reasonable for most practical applications.

The difficulty of implementing these control techniques can vary depending on the level of expertise and experience of the control engineer. The hybrid control strategy and OGY method require a good understanding of control theory, nonlinear dynamics, and feedback control. However, with proper training and experience, these methods can be implemented effectively.

In practical applications, the cost of implementing a control strategy must be balanced against the benefits it provides. If the cost of implementing the control strategy is too high, it may reduce the practical significance of eliminating chaotic behavior. Therefore, it is essential to carefully evaluate the specific system, and the control method is used to determine its practical significance.

Hybrid control strategy is applied to system (2) controlling chaos. We rewrite our uncontrolled system (2) as

$$X_{n+1} = G(X_n, \delta), \tag{59}$$

where $X_n \in \mathbb{R}^3$, $G(.)$ is nonlinear vector function, and $\delta \in \mathbb{R}$ is bifurcation parameter. Applying hybrid control strategy, the controlled system of (59) becomes

$$X_{n+1} = \rho G(X_n, \delta) + (1 - \rho) X_n, \tag{60}$$

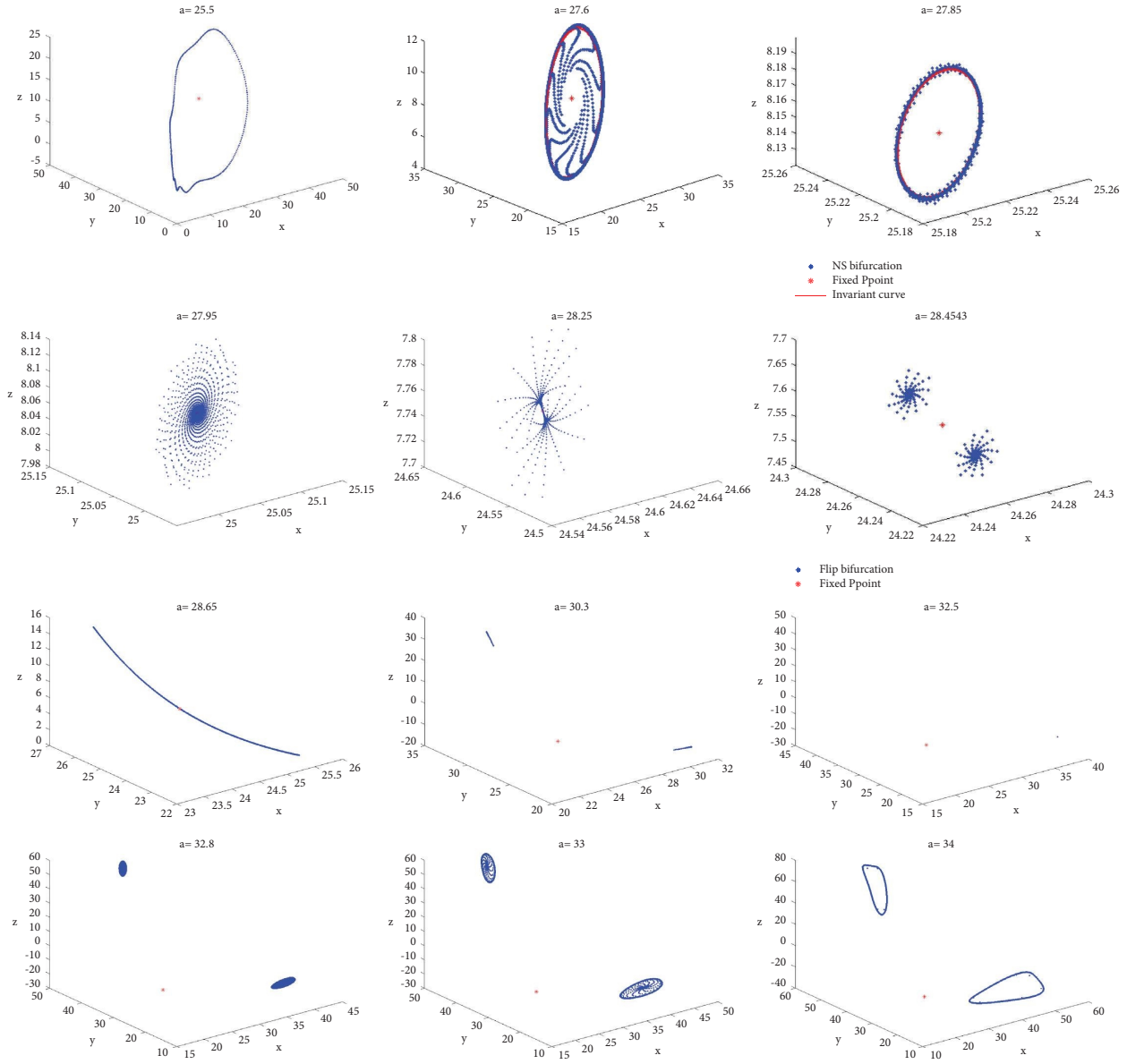

Figure 8: Phase portrait for different values of **a** corresponding to Figures 7(a)–7(c). Red $*$ is the fixed point E_+.

where $0 < \rho < 1$ is the control parameter. Now, if we implement the above mentioned control strategy to system (2), then we get the following controlled system:

$$\begin{cases} x_{n+1} = \rho\left(x_n + \delta\left(a\left(y_n - x_n\right)\right)\right) + (1-\rho)x_n, \\ y_{n+1} = \rho\left(y_n + \delta\left((c-a)x_n - x_n z_n + c y_n\right)\right) + (1-\rho)y_n, \\ z_{n+1} = \rho\left(z_n + \delta\left(x_n y_n - b z_n\right)\right) + (1-\rho)z_n. \end{cases} \tag{61}$$

For the controlled system (61), the Jacobian matrix at fixed point $E_+(x^+, y^+, z^+)$ (which is a fixed point of system (2)) takes the following form:

$$J\left(E_+\right) = \begin{pmatrix} 1 - a\delta\rho & a\delta\rho & 0 \\ -\left(a - c + z^+\right)\delta\rho & 1 + c\delta\rho & -x^+\delta\rho \\ y^+\delta\rho & x^+\delta\rho & 1 - b\delta\rho \end{pmatrix}. \tag{62}$$

Then, the zeroes of $|\mu I - J(E_+)|$ (eigenvalues of J) satisfy the equation

$$\mu^3 + \varepsilon_2\mu^2 + \varepsilon_1\mu + \varepsilon_0 = 0, \tag{63}$$

where

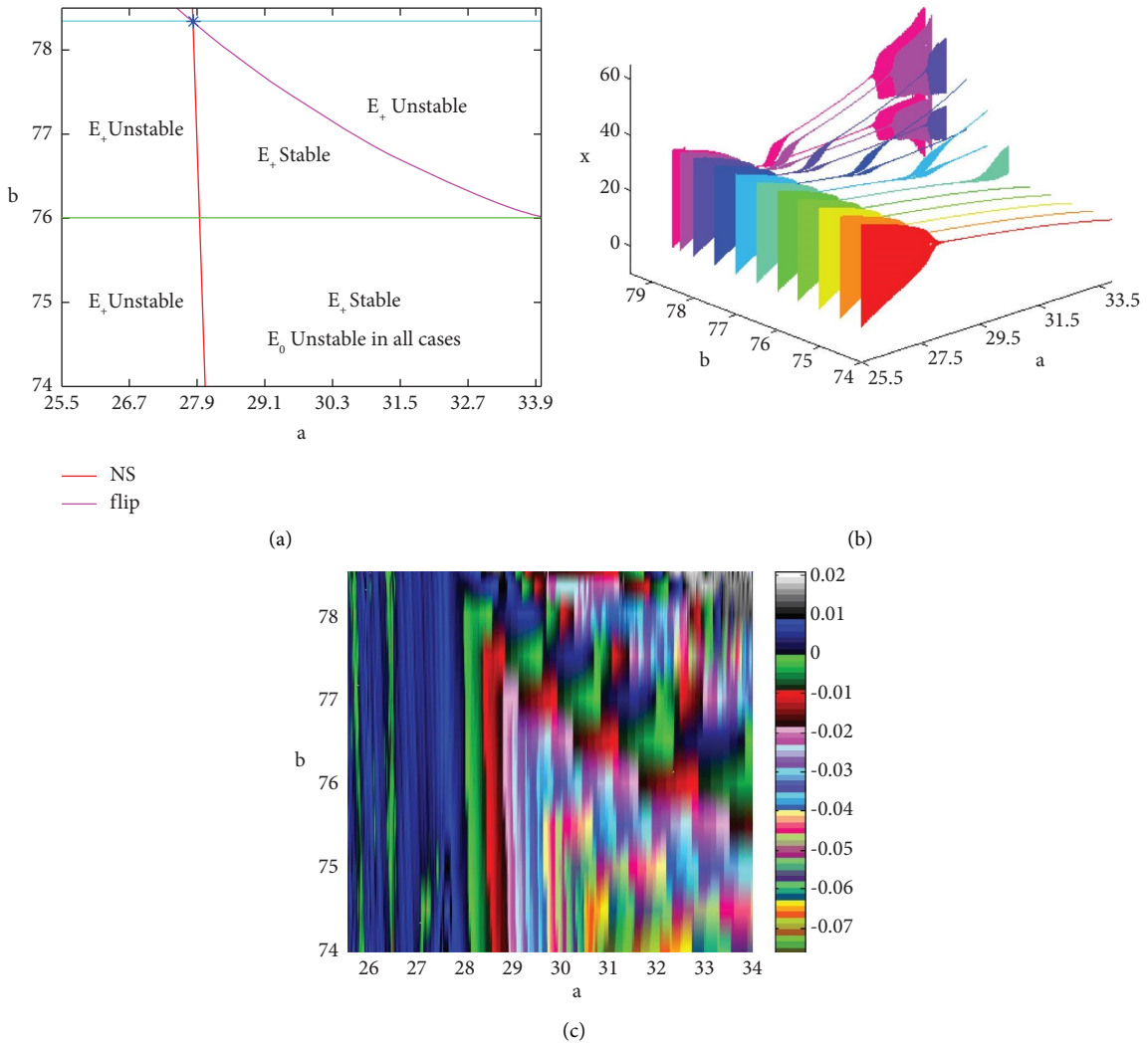

FIGURE 9: System dynamics for control parameters a and b: (a) stability region with flip-NS bifurcation curve, (b) bifurcation diagram in (a, b, x) space for $a \in [25.5, 34]$ and $b = 74.5, 75, 75.5, 76, 76.5, 77, 77.5, 78, 78.3301, 78.5 \in [74, 79]$, and (c) the projection of MLEs onto (a, b) plane.

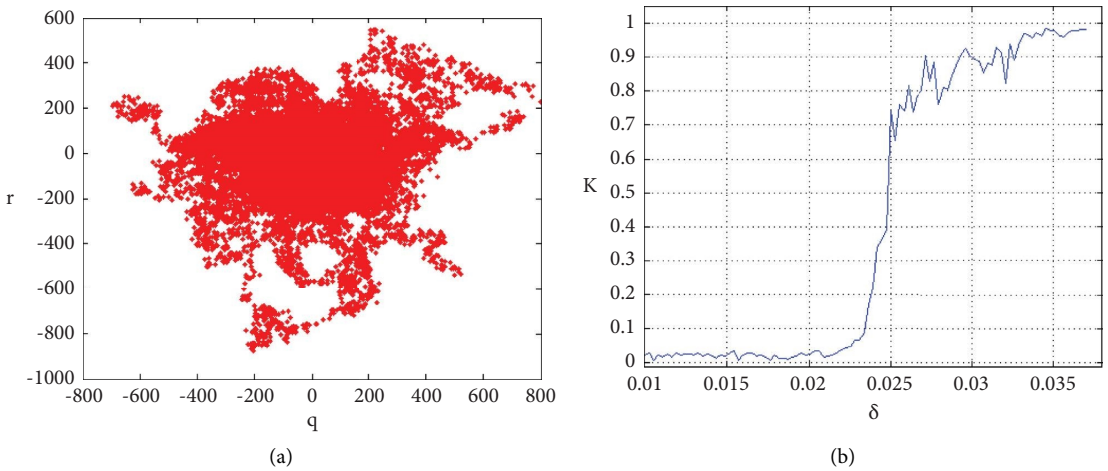

FIGURE 10: 0 – 1 chaos test for system (2). (a) K versus δ and (b) plot in new coordinates (q, r) plane with $\delta = 0.037$.

$$\begin{aligned}
\varepsilon_2 &= -3 + \delta\rho(a + b - c),\\
\varepsilon_1 &= 3 + 2c\delta\rho + a^2\delta^2\rho^2 + x^{+2}\delta^2\rho^2 - b\delta\rho(2 + c\delta\rho) + a\delta\rho\left(-2 + \delta\rho\left(b - 2c + z^{+}\right)\right),\\
\varepsilon_0 &= -1 - c\delta\rho - x^{+2}\delta^2\rho^2 + a^2\delta^2\rho^2(-1 + b\delta\rho) + b\delta\rho(1 + c\delta\rho)\\
&\quad + a\delta\rho\Big(1 + \delta\rho\left(2c - z^{+}\right) + \delta^2\rho^2\left(x^{+2} + x^{+}y^{+}\right) - b\delta\rho\left(1 + \delta\rho\left(2c - z^{+}\right)\right)\Big).
\end{aligned} \tag{64}$$

Lemma 16. *If the fixed point $E_+(x^+, y^+, z^+)$ of the uncontrolled system (2) is unstable, then it is a sink (stable) for the controlled system (61) if the roots of (63) lie inside open disk satisfying conditions in Lemma 1.*

Example 17. To determine whether a hybrid control method is effective at containing chaotic (unstable) system dynamics, we fix $a = 28, b = 55, c = 18$ with $\delta = 0.037 > \delta_{NS}$. This therefore demonstrates that the fixed point $E_+(20.9762, 20.9762, 8)$ of system (2) is unstable (see Figure 6); however, the controlled system (61) is stable at this set position iff $0 < \rho < 0.59584488$. Taking $\rho = 0.4$, the unstable system dynamics around E_+ are eliminated showing that E_+ is a sink for the controlled system (61) which have been displayed in Figure 11(b), and time series of the controlled system (61) is displayed in Figure 11(a).

Next, we apply OGY approach in [42] to control the Chen system's chaotic motion on the stable period −1 orbit. Assume that a is the control parameter which somewhat perturbed over time and that system (2) is stated as in (59):

$$X_{i+1} = G(X_i, a), X_i \in R^3, a \in R. \tag{65}$$

Let $X^{**}(\tilde{a})$ indicate the unstable equilibrium point. Using the Taylor first-order expansion, the system (2) can be written as

$$X_{i+1} - X^{**}(\tilde{a}) = \widetilde{A}\left(X_i - X^{**}(\tilde{a})\right) + \widetilde{B}(a - \tilde{a}), \tag{66}$$

where $\widetilde{A}$ is the Jacobian matrix of $G(X, a)$ with respect to the set of variables $X = (x, y, z)$,

$$\begin{aligned}
\widetilde{A} &= D_X G(X, a)\\
&= \begin{pmatrix} 1 - a\delta & a\delta & 0\\ -(a - c + z)\delta & 1 + c\delta & -x\delta\\ y\delta & x\delta & 1 - b\delta \end{pmatrix},
\end{aligned} \tag{67}$$

and $\widetilde{B}$ is the derivative matrix of $G(X, a)$ to the variable a,

$$\begin{aligned}
\widetilde{B} &= D_a G(X, a)\\
&= \begin{pmatrix} -(x + y)\delta\\ -x\delta\\ 0 \end{pmatrix}.
\end{aligned} \tag{68}$$

Put the parameter values $b = 78, c = 18, \tilde{a} = 25.5$, $\delta = 0.0264$ and the fixed point $E_+(28.6182, 28.6182, 10.5)$ in the matrices $\widetilde{A}$ and $\widetilde{B}$:

$$\begin{aligned}
\widetilde{A} &= \begin{pmatrix} 0.3268 & 0.6732 & 0\\ -0.4752 & 1.4752 & -0.75552\\ 0.75552 & 0.75552 & -1.0592 \end{pmatrix},\\
\widetilde{B} &= \begin{pmatrix} 0\\ -0.75552\\ 0 \end{pmatrix}.
\end{aligned} \tag{69}$$

We define the control parameter a in the following form:

$$a - \tilde{a} = -\widehat{K}^T\left(X_i - X^{**}(\tilde{a})\right). \tag{70}$$

Then, (67) becomes

$$X_{i+1} - X^{**}(\tilde{a}) = \left(\widetilde{A} - \widetilde{B}\widehat{K}^T\right)\left(X_i - X^{**}(\tilde{a})\right). \tag{71}$$

The fixed point $X^{**}(\tilde{a})$ will be a sink is the eigenvalues of $\widetilde{A} - \widetilde{B}\widehat{K}^T$ lie in the unit disc. We can determine the $C_{3\times3}$ control matrix as follows:

$$\begin{aligned}
C &= \left(\widetilde{B}\ \ \widetilde{A}\widetilde{B}\ \ \widetilde{A}^2\widetilde{B}\right)\\
&= \begin{pmatrix} 0 & -0.508616 & -0.916526\\ -0.75552 & -1.11454 & -0.971221\\ 0 & -0.57081 & -0.621727 \end{pmatrix}.
\end{aligned} \tag{72}$$

To stabilize the chaotic trajectories into stable periodic orbit and to get the solution of the pole placement, we set the matrix

$$\widehat{K}^T = (\hat{\alpha}_3 - \hat{a}_3, \hat{\alpha}_2 - \hat{a}_2, \hat{\alpha}_1 - \hat{a}_1)Q^{-1}, \tag{73}$$

and $Q = CP$, where P is a matrix of order 3

$$P = \begin{pmatrix} a_2 & a_1 & 0\\ a_1 & 1 & 0\\ 1 & 0 & 0 \end{pmatrix}. \tag{74}$$

In (73), $\hat{a}_i\,(i = 1, 2, 3)$ are the coefficients of the characteristic equation of $\widetilde{A}$:

$$\begin{aligned}
&\lambda^3 - 0.7428\lambda^2 - 0.535868\lambda + 1.04721\\
&\quad = 0 = \lambda^3 + \hat{a}_1\lambda^2 + \hat{a}_2\lambda + \hat{a}_3,
\end{aligned} \tag{75}$$

and $\hat{\alpha}_i\,(i = 1, 2, 3)$ are the coefficients of the characteristic equation of the matrix

$$\widetilde{A} - \widetilde{B}\widehat{K}^T = \begin{pmatrix} 0.3268 & 0.6732 & 0\\ -3.91752 & 1.6903 & -0.479795\\ 0.75552 & 0.7552 & -1.0592 \end{pmatrix}, \tag{76}$$

which is defined as

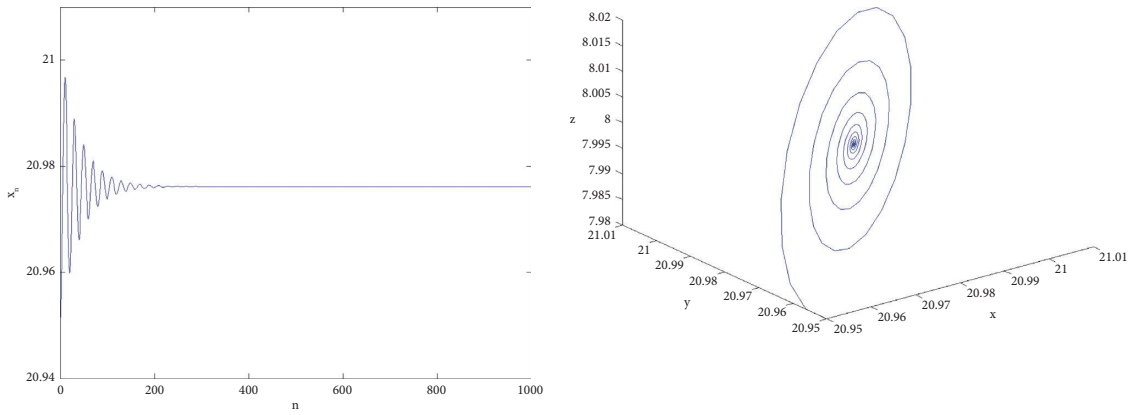

(a) (b)

Figure 11: Controlling chaos of system (61): (a) time history of x and (b) phase diagram of system (61).

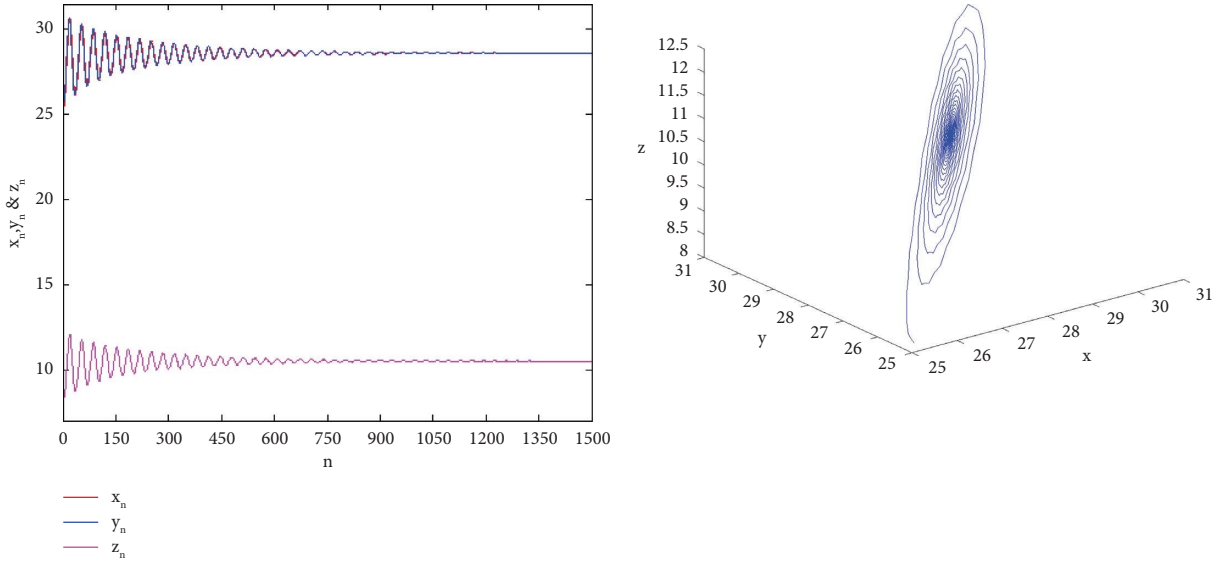

(a) (b)

Figure 12: Controlling the system (66)'s chaos: (a) time history of x, y, z and (b) phase diagram of system (66).

$$\mu_a^3 - 0.9579\mu_a^2 - 0.9579\mu_a - 0.99 = 0 = \mu_a^3 + \widehat{\alpha}_1\mu_a^2 + \widehat{\alpha}_2\mu_a + \widehat{\alpha}_3. \tag{77}$$

Now, the matrix Q becomes

$$\begin{aligned} Q &= \begin{pmatrix} 0 & -0.508616 & -0.916526 \\ -0.75552 & -1.11454 & -0.971221 \\ 0 & -0.57081 & -0.621727 \end{pmatrix} \cdot \begin{pmatrix} -0.535868 & -0.7428 & 1 \\ -0.7428 & 1 & 0 \\ 1 & 0 & 0 \end{pmatrix} \\ &= \begin{pmatrix} -0.538726 & -0.508616 & 0 \\ 0.261521 & -0.553343 & -0.75552 \\ -0.197729 & -0.57081 & 0 \end{pmatrix}, \\ Q^{-1} &= \begin{pmatrix} -2.75831 & 0 & 2.45777 \\ 0.955477 & 2.22045 \times 10^{-16} & -2.60327 \\ -1.65457 & -1.32359 & 2.75738 \end{pmatrix}. \end{aligned} \tag{78}$$

Therefore, from (73), the matrix $\widehat{K}^T$ is given by $\widehat{K}^T = (0.110451, 0.284705, 0.364947)$. Figure 12 shows how the aforementioned chaos management strategy works in practice.

6. Conclusion

We present a qualitative analysis of the Chen system in discrete time. We explicitly find the conditions and directions of the NS bifurcation of system (2) in the vicinity of the fixed point E_0. Then, we find the existence criteria of the PD and NS bifurcations of system (2) around a fixed point E_+. In addition, the directions of both bifurcations are given by the center manifold theory. More specifically, we notice that system (2) emerges with a PD bifurcation around E_0 and a PD or NS bifurcation around E_+ when the parameters δ and a vary in a small vicinity of their critical values. For the mechanism of both bifurcations, the dynamics of system (2) switches from stable state to unstable state and triggers a route to chaos and vice versa. When the topological properties of system (2) change through a PD bifurcation, we obtain period $-2, -8$ orbits and two coexisting attracting chaotic sets. When the topological properties of system (2) change through a NS bifurcation, we find a closed invariant curve that attracts chaotic sets. From Figure 9, we find that system (2) experiences both bifurcations when $b > 76$ (approx.). We present the 3D bifurcation diagrams to see how the PD and NS bifurcation advance or delay when two parameters change its value. In all cases, the dynamic complexities of system (2) are justified with the sign of MLEs. We also use the $0-1$ test algorithm for chaos to detect whether there is chaos in the system or not. Finally, we are able to eliminate chaotic dynamics by applying a hybrid control strategy and the OGY method. For this discrete system, it is open to study the other properties such as synchronization and codimension-2 bifurcation.

Data Availability

The data presented in this study are intended solely for illustrative purposes and are not based on actual observations.

Conflicts of Interest

The authors declare that they have no conflicts of interest.

Authors' Contributions

All authors contributed equally to carry out the proof of the main results and approved the final manuscript.

References

[1] J. Kengne, Z. T. Njitacke, and H. B. Fotsin, "Dynamical analysis of a simple autonomous jerk system with multiple attractors," *Nonlinear Dynamics*, vol. 83, no. 1, pp. 751–765, 2016.

[2] E. N. Lorenz, "Deterministic nonperiodic flow," *Journal of the Atmospheric Sciences*, vol. 20, no. 2, pp. 130–141, 1963.

[3] J. Lü, G. Chen, and S. Zhang, "Dynamical analysis of a new chaotic attractor," *International Journal of Bifurcation and chaos*, vol. 12, no. 5, pp. 1001–1015, 2002.

[4] W. Luo, Q. Ou, Y. Fei, L. Cui, and J. Jin, "Analysis of a new hidden attractor coupled chaotic system and application of its weak signal detection," *Mathematical Problems in Engineering*, vol. 2020, Article ID 8849283, 15 pages, 2020.

[5] T. Ueta and G. Chen, "Bifurcation analysis of chen's equation," *International Journal of Bifurcation and Chaos*, vol. 10, no. 08, pp. 1917–1931, 2000.

[6] P. Chakraborty, S. Sarkar, and U. Ghosh, "Stability and bifurcation analysis of a discrete prey–predator model with sigmoid functional response and allee effect," *Rendiconti del Circolo Matematico di Palermo Series 2*, vol. 70, pp. 253–273, 2020.

[7] E. M. Elabbasy, A. A. Elsadany, and Y. Zhang, "Bifurcation analysis and chaos in a discrete reduced lorenz system," *Applied Mathematics and Computation*, vol. 228, pp. 184–194, 2014.

[8] L. Fei, X. Chen, and B. Han, "Bifurcation analysis and hybrid control of a discrete-time predator–prey model," *Journal of Difference Equations and Applications*, vol. 27, no. 1, pp. 102–117, 2021.

[9] J. Huang, S. Liu, S. Ruan, and D. Xiao, "Bifurcations in a discrete predator–prey model with nonmonotonic functional response," *Journal of Mathematical Analysis and Applications*, vol. 464, no. 1, pp. 201–230, 2018.

[10] P. K. Santra and G. S. Mahapatra, "Dynamical study of discrete-time prey–predator model with constant prey refuge under imprecise biological parameters," *Journal of Biological Systems*, vol. 28, no. 3, pp. 681–699, 2020.

[11] F. Kangalgil and S. Kartal, "Stability and bifurcation analysis in a host-parasitoid model with hassell growth function," *Advances in Difference Equations*, vol. 2018, no. 1, pp. 240–315, 2018.

[12] B. Li and Q. He, "Bifurcation analysis of a two-dimensional discrete hindmarsh–rose type model," *Advances in Difference Equations*, vol. 2019, no. 1, pp. 124–217, 2019.

[13] Y. Liu and X. Li, "Dynamics of a discrete predator-prey model with holling-ii functional response," *International Journal of Biomathematics*, vol. 14, Article ID 2150068, 2021.

[14] S. M. Rana and U. Kulsum, "Bifurcation analysis and chaos control in a discrete-time predator-prey system of leslie type with simplified holling type iv functional response," *Discrete Dynamics in Nature and Society*, vol. 2017, Article ID 9705985, 11 pages, 2017.

[15] S. M. S. Rana, "Dynamics and chaos control in a discrete-time ratio-dependent holling-tanner model," *Journal of the Egyptian Mathematical Society*, vol. 27, no. 1, pp. 1–16, 2019.

[16] A. Singh and P. Deolia, "Bifurcation and chaos in a discrete predator–prey model with holling type-iii functional response and harvesting effect," *Journal of Biological Systems*, vol. 29, no. 02, pp. 451–478, 2021.

[17] J. Wang and G. Feng, "Bifurcation and chaos in discrete-time bvp oscillator," *International Journal of Non-linear Mechanics*, vol. 45, no. 6, pp. 608–620, 2010.

[18] Y. Zhang, C. Qi, and S. Deng, "Qualitative structure of a discrete predator-prey model with nonmonotonic functional response," *Discrete & Continuous Dynamical Systems-S*, vol. 16, 2022.

[19] M. Zhao, "Bifurcation and chaotic behavior in the discrete bvp oscillator," *International Journal of Non-linear Mechanics*, vol. 131, Article ID 103687, 2021.

[20] G. S. Mahapatra, P. K. Santra, and E. Bonyah, "Dynamics on effect of prey refuge proportional to predator in discrete-time prey-predator model," *Complexity*, vol. 2021, Article ID 6209908, 12 pages, 2021.

[21] M. Berkal and M. B. Almatrafi, "Bifurcation and stability of two-dimensional activator–inhibitor model with fractional-

order derivative," *Fractal and Fractional*, vol. 7, no. 5, p. 344, 2023.

[22] A. Q. Khan, S. A. H. Bukhari, and M. B. Almatrafi, "Global dynamics, neimark-sacker bifurcation and hybrid control in a leslie's prey-predator model," *Alexandria Engineering Journal*, vol. 61, no. 12, Article ID 11391, 2022.

[23] A. Q. Khan, F. Nazir, and M. B. Almatrafi, "Bifurcation analysis of a discrete phytoplankton–zooplankton model with linear predational response function and toxic substance distribution," *International Journal of Biomathematics*, vol. 16, no. 4, Article ID 2250095, 2023.

[24] M. A. Abdelaziz, A. I. Ismail, F. A. Abdullah, and M. H. Mohd, "Codimension one and two bifurcations of a discrete-time fractional-order seir measles epidemic model with constant vaccination," *Chaos, Solitons & Fractals*, vol. 140, Article ID 110104, 2020.

[25] F. Guo, Y. Ding, and J. Li, "Neimark–sacker bifurcation and controlling chaos in a three-species food chain model through the ogy method," *Discrete Dynamics in Nature and Society*, vol. 2021, Article ID 6316235, 13 pages, 2021.

[26] Z. Hu, Z. Teng, and L. Zhang, "Stability and bifurcation analysis in a discrete sir epidemic model," *Mathematics and Computers in Simulation*, vol. 97, pp. 80–93, 2014.

[27] I. Waqas, Q. Din, M. Taj, and M. A. Iqbal, "Bifurcation and chaos control in a discrete-time predator–prey model with nonlinear saturated incidence rate and parasite interaction," *Advances in Difference Equations*, vol. 2019, no. 1, pp. 1–16, 2019.

[28] M. S. Khan, M. Ozair, T. Hussain, J. F. Gómez-Aguilar, and M. Samreen, "Bifurcation analysis of a discrete-time compartmental model for hypertensive or diabetic patients exposed to covid-19," *The European Physical Journal Plus*, vol. 136, no. 8, pp. 1–26, 2021.

[29] S. Qin, J. Zhang, W. Du, and J. Yu, "Neimark–sacker bifurcation in a new three–dimensional discrete chaotic system," *ICIC-EL*, vol. 10, no. 4, pp. 1–7, 2016.

[30] B. Xin, T. Chen, and J. Ma, "Neimark-sacker bifurcation in a discrete-time financial system," *Discrete Dynamics in Nature and Society*, vol. 2010, Article ID 405639, 12 pages, 2010.

[31] S. M. S. Rana and M. J. Uddin, "Dynamics of a discrete-time chaotic lü system," *Pan-American Journal of Mathematics*, vol. 1, no. 7, p. 7, 2022.

[32] A. Q. Khan, M. Tasneem, and M. B. Almatrafi, "Discrete-time covid-19 epidemic model with bifurcation and control," *Mathematical Biosciences and Engineering*, vol. 19, no. 2, pp. 1944–1969, 2021.

[33] C. Sparrow, *The Lorenz Equations: Bifurcations, Chaos, and Strange Attractors*, Vol. 41, Springer Science and Business Media, New York, NY, USA, 2012.

[34] C. Elias and G. Ladas, *Dynamics of Third-Order Rational Difference Equations with Open Problems and Conjectures*, Vol. 5, CRC Press, Boca Raton, FL, USA, 2007.

[35] Y. A. Kuznetsov, *Elements of Applied Bifurcation Theory*, Vol. 112, Springer Science and Business Media, New York, USA, 2013.

[36] G. Wen, "Criterion to identify hopf bifurcations in maps of arbitrary dimension," *Physical Review*, vol. 72, no. 2, Article ID 026201, 2005.

[37] S. Yao, "New bifurcation critical criterion of flip-neimark-sacker bifurcations for two-parameterized family of-dimensional discrete systems," *Discrete Dynamics in Nature and Society*, vol. 2012, 2012.

[38] G. A. Gottwald and I. Melbourne, "A new test for chaos in deterministic systems," *Proceedings of the Royal Society of London. Series A: Mathematical, Physical and Engineering Sciences*, vol. 460, no. 2042, pp. 603–611, 2004.

[39] B. Xin and Y. Li, "0-1 test for chaos in a fractional order financial system with investment incentive," *Abstract and Applied Analysis*, vol. 2013, Article ID 876298, 10 pages, 2013.

[40] B. Xin and Z. Wu, "Neimark–sacker bifurcation analysis and 0–1 chaos test of an interactions model between industrial production and environmental quality in a closed area," *Sustainability*, vol. 7, no. 8, Article ID 10191, 2015.

[41] L.-G. Yuan and Q.-G. Yang, "Bifurcation, invariant curve and hybrid control in a discrete-time predator–prey system," *Applied Mathematical Modelling*, vol. 39, no. 8, pp. 2345–2362, 2015.

[42] A. Alasty and H. Salarieh, "Nonlinear feedback control of chaotic pendulum in presence of saturation effect," *Chaos, Solitons & Fractals*, vol. 31, no. 2, pp. 292–304, 2007.